On the PDF Frontier

Pavel Nadolsky

Southern Methodist University

Dallas, TX, USA

Based on studies with CTEQ-TEA and PDF4LHC working groups

September 12, 2016

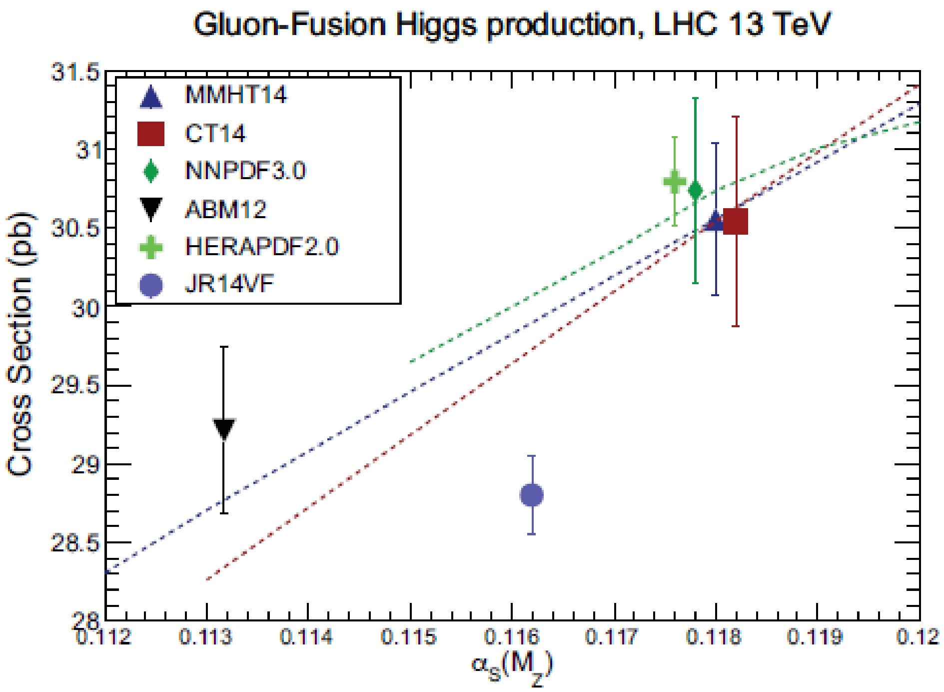

ON ~~AT~~ THE PDF FRONTIER: CTEQ (TUNG ET AL.)

- Introduction to modern parton distribution functions (PDFs)
- Latest developments associated with PDFs

PAVEL NADOLSKY
(SMU)

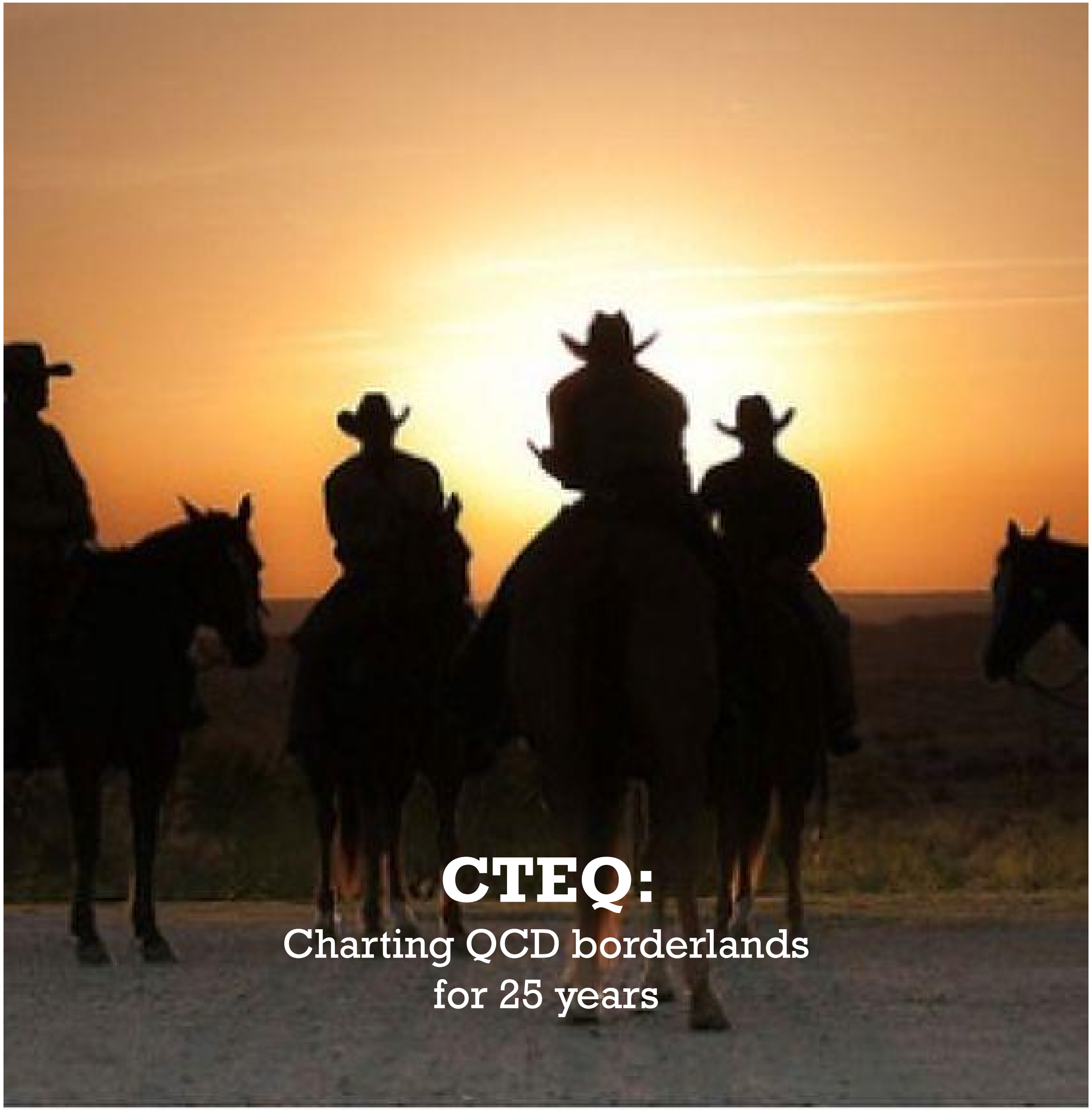

CTEQ-TEA (CT)

Southern Methodist U.:
T.-J. Hou, P.N. , B. Wang, K. Xie

SMU/Argonne/Jiaotong:
J. Gao

U. Manchester: M.Guzzi

Michigan State U.:
J. Huston, J. Pumplin, C. Schmidt, D. Stump, C. -P. Yuan

Xinjiang: S. Dulat

+CTEQ-JLAB (CJ)

Global analysis *(term promoted by J. Morfin & W.-K. Tung in 1990)*:

constrains PDFs or other nonperturbative functions with data from diverse hadronic experiments

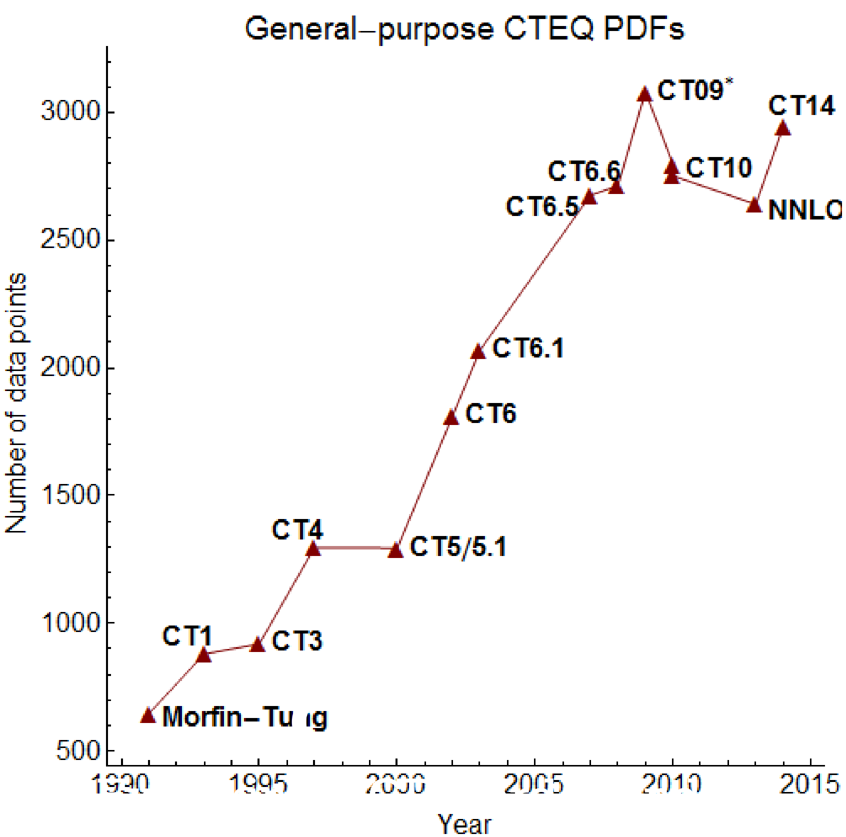

Morfin–Tung:	DIS, low–Q Drell–Yan process
CT1:	DIS, DY, direct γ
CT3:	low–x DIS, W charge asymmetry
CT4:	– direct γ; + CDF high–p_T jets
CT5/5.1:	$+\sigma_{pp}/\sigma_{pd}$ in DY process; D0 jets
CT6:	Error PDFs; correlated syst. errors
CT6.1:	Tevatron Run–1b jets
CT6.5:	GM–VFN scheme; free s(x)
CT6.6:	PDF correlations
CT09*:	+Tevatron Run–2 jets
CT10:	+NNLO, combined HERA, Run–2 W asymmetry
CT14:	+LHC Run–1 W, Z, jet production

THE INNER WORLD OF A HADRON

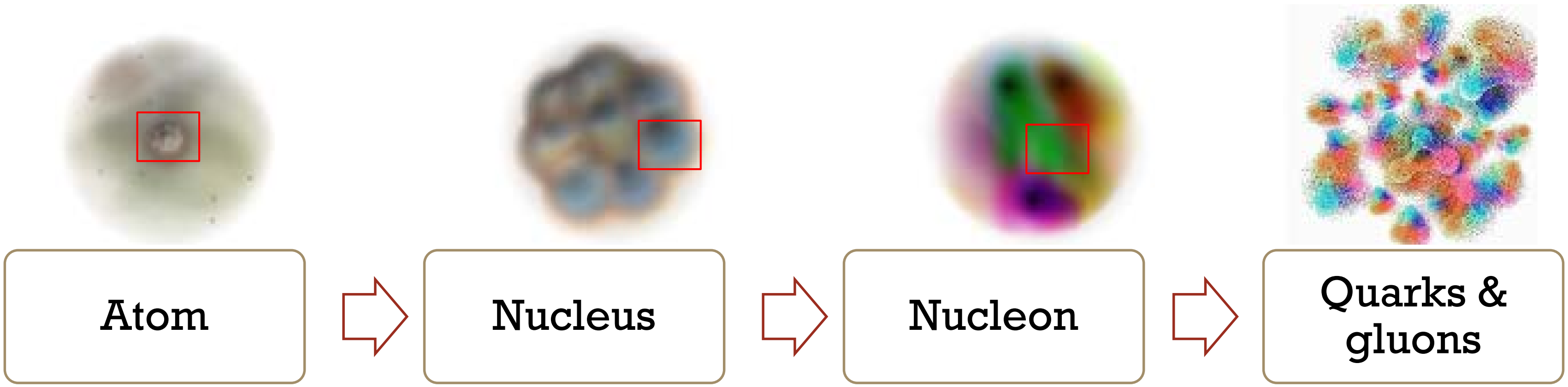

The structure of the hadron drastically changes as the resolution of the "microscope" (scattering process) increases

THE INNER WORLD OF A HADRON

Atom → Nucleus → Nucleon → Quarks & gluons

Unpolarized collinear parton distributions $f_{a/p}(x,Q)$ are associated with probabilities for finding a parton a with the "+" momentum component xp^+ in a proton with the "+" component p^+, at a resolution scale Q, for $p^+ \to \infty$

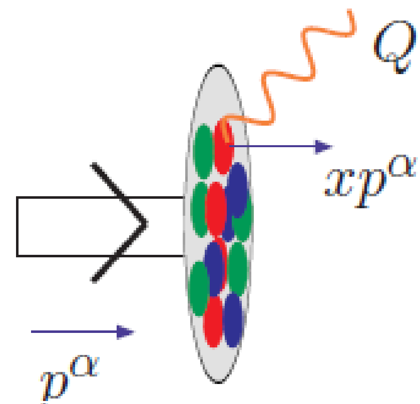

Parton distribution functions $f_{a/p}(x, Q)$...

... the best-known nonperturbative functions introduced in QCD

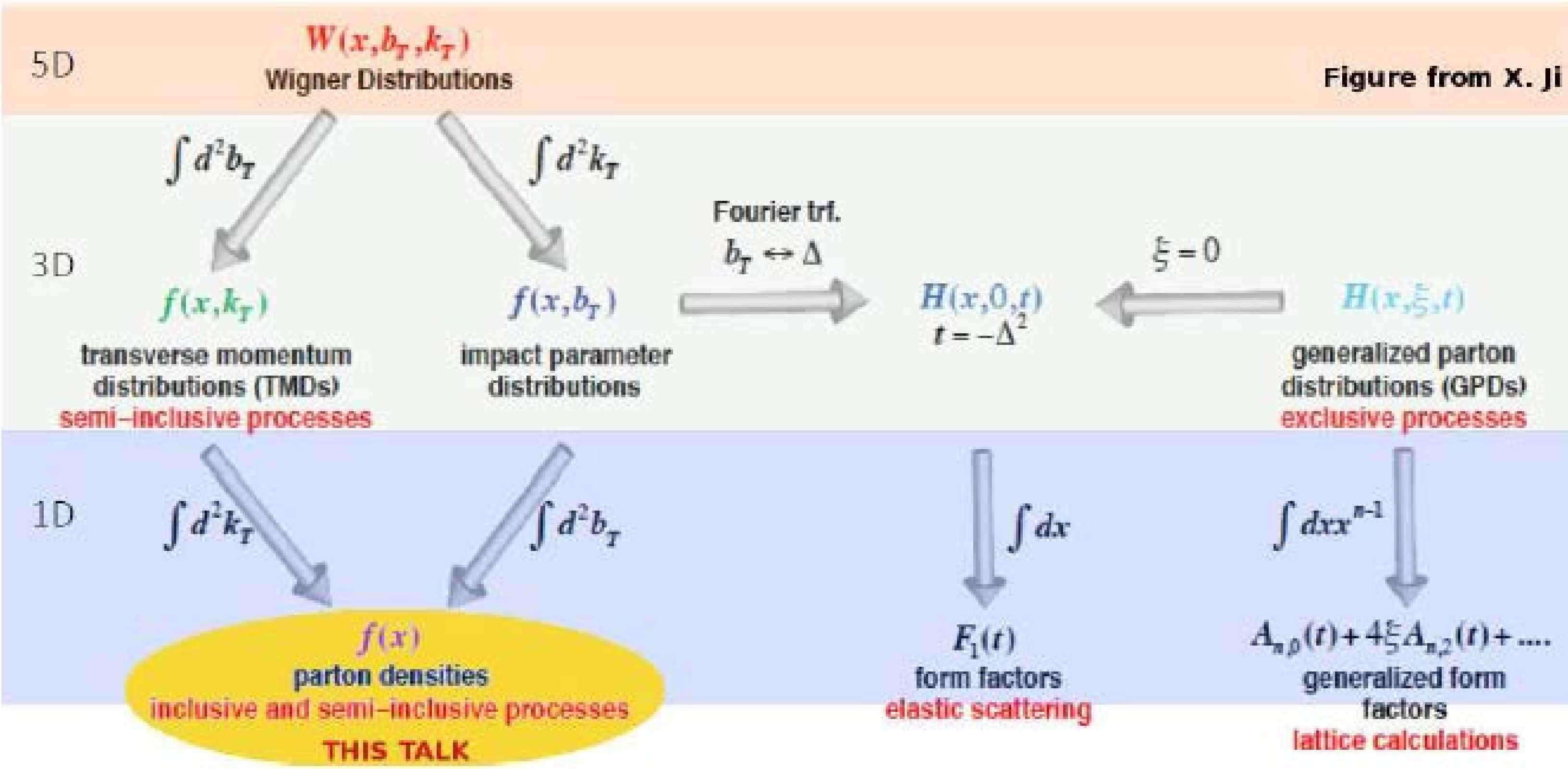

... can be obtained from most general Wigner distribution functions $W_a(x^\alpha, p^\beta, s^\gamma)$

EXAMPLE: TOTAL CROSS SECTION FOR gg → Higgs → $\gamma\gamma$

Cross section $\sigma_{pp\to H\to\gamma\gamma}$ for production and decay of H, e.g., via $g+g\to H$:

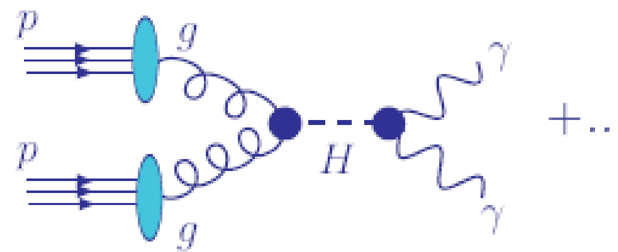

$$\sigma_{pp\to H\to\gamma\gamma X}(Q) = \sum_{a,b=g,q,\bar{q}} \int_0^1 d\xi_a \int_0^1 d\xi_b \hat{\sigma}_{ab\to H\to\gamma\gamma}\left(\frac{x_a}{\xi_a},\frac{x_b}{\xi_b},\frac{Q}{\mu_R},\frac{Q}{\mu_F};\alpha_s(\mu_R)\right)$$
$$\times f_a(\xi_a,\mu_F) f_b(\xi_b,\mu_F) + O\left(\frac{\Lambda_{QCD}^2}{Q^2}\right)$$

- $\hat{\sigma}_{ab\to H\to\gamma\gamma}$ is the cross section for scattering of two partons, a and b; can be computed as a **perturbative** series in $\alpha_s(\mu_R)$, at a renormalization scale $\mu_R \gg \Lambda_{QCD}$

- $f_{a/p}\,(\xi,\mu_F)$ is the **nonperturbative** PDF for finding a parton a with the momentum fraction ξ in the proton p, at a factorization scale $\mu_F \gg \Lambda_{QCD}$

HARD-SCATTERING CROSS SECTIONS FOR $gg \to H \to \gamma\gamma$

N3LO for total cross sections

NNLO for differential distributions

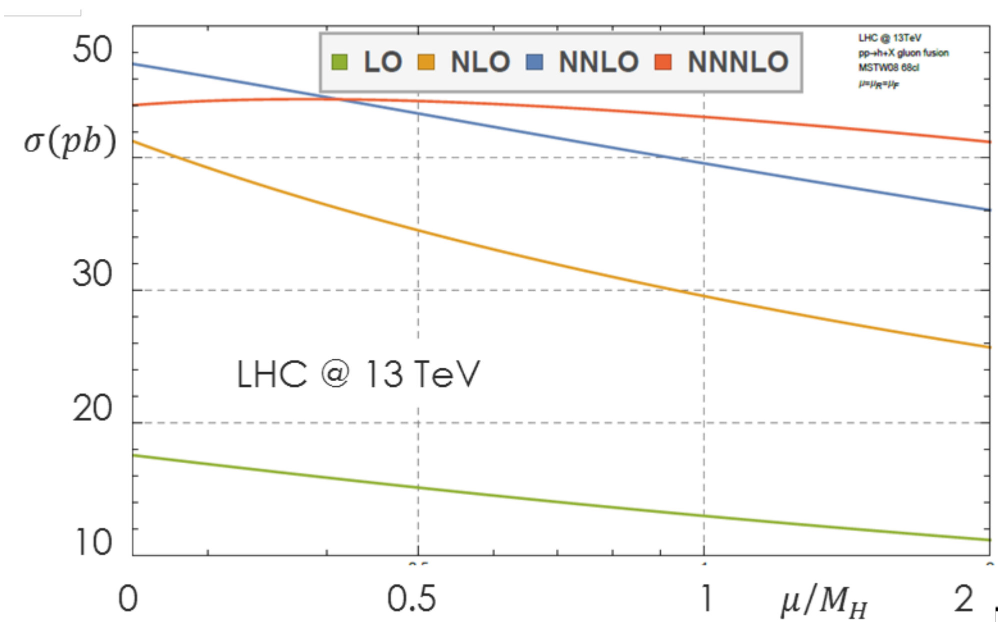

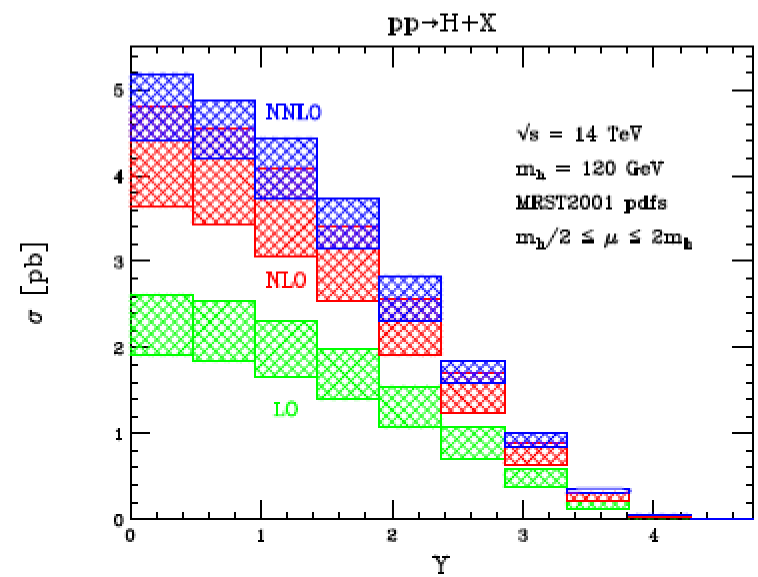

Anastasiou, Duhr, Dulat, Herzog, Mistlberger, 1503.06056

N3LO corrections are of the order of +2.2%. The total scale variation at N3LO is 3%

Anastasiou, Melnikov, Petriello, hep-ph/0409088, 0501130

PERTURBATIVE QCD LOOP REVOLUTION

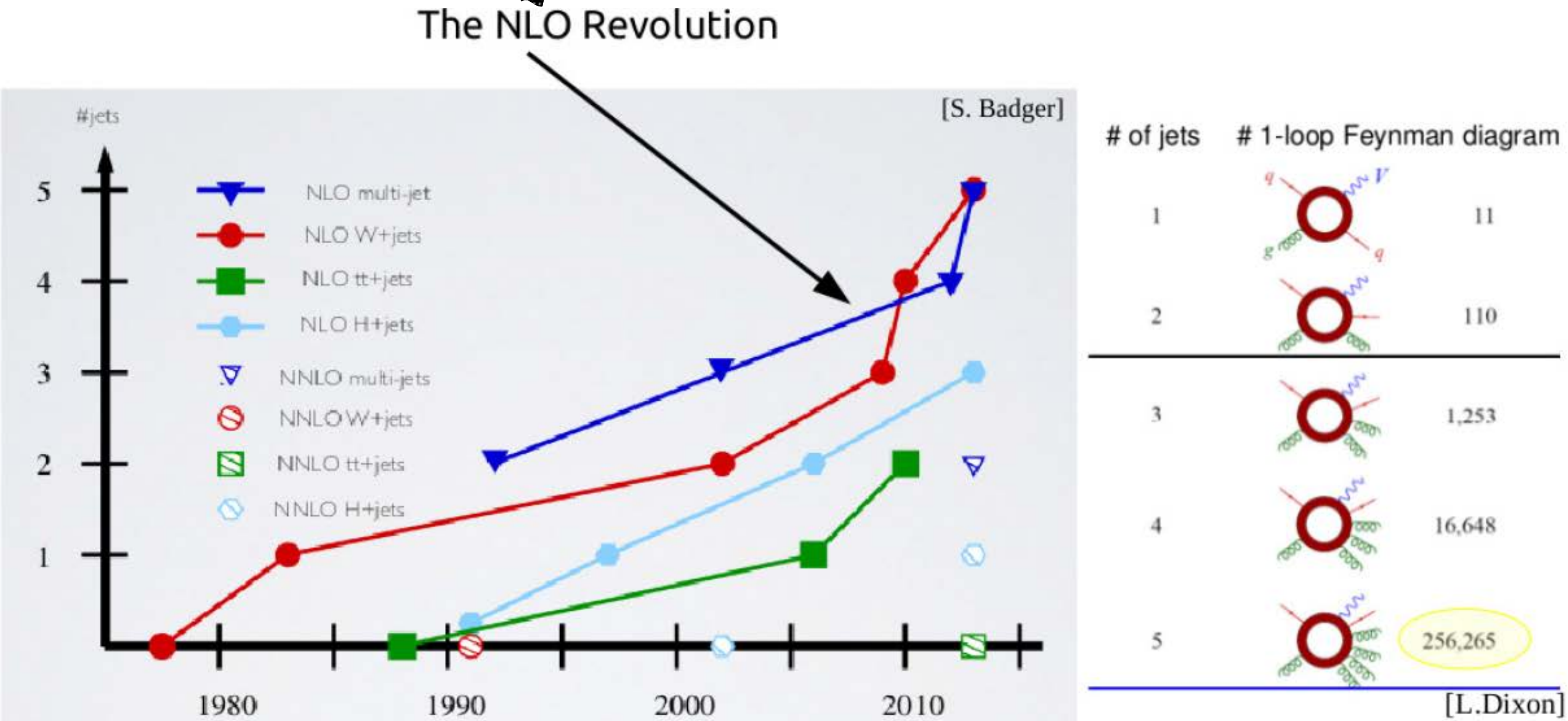

Since 2005, generalized unitarity, sector decomposition, and related methods dramatically advanced the computations of **perturbative** NLO/NNLO/N3LO hard cross sections.

To make use of it, PDF accuracy must keep up

General-purpose CT14 PDFs

(S. Dulat et al., arXiv:1506.07443)

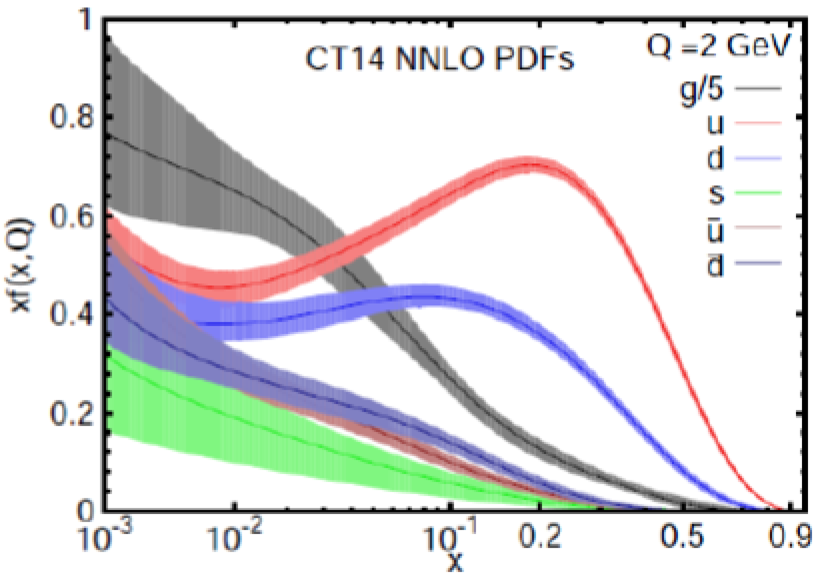

Q= 2 GeV

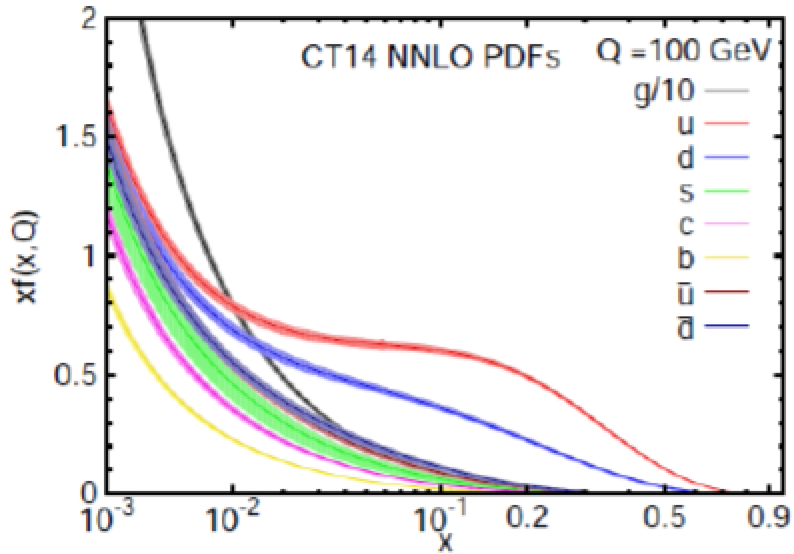

Q= 100 GeV

Phenomenological parametrizations of PDFs are provided with estimated uncertainties of multiple origins (**uncertainties of measurement, theoretical model, parametrization form, statistical analysis**, …)

The shape of PDFs is optimized w.r.t. hundreds of **nuisance parameters**

FRONTIERS OF THE PDF ANALYSIS

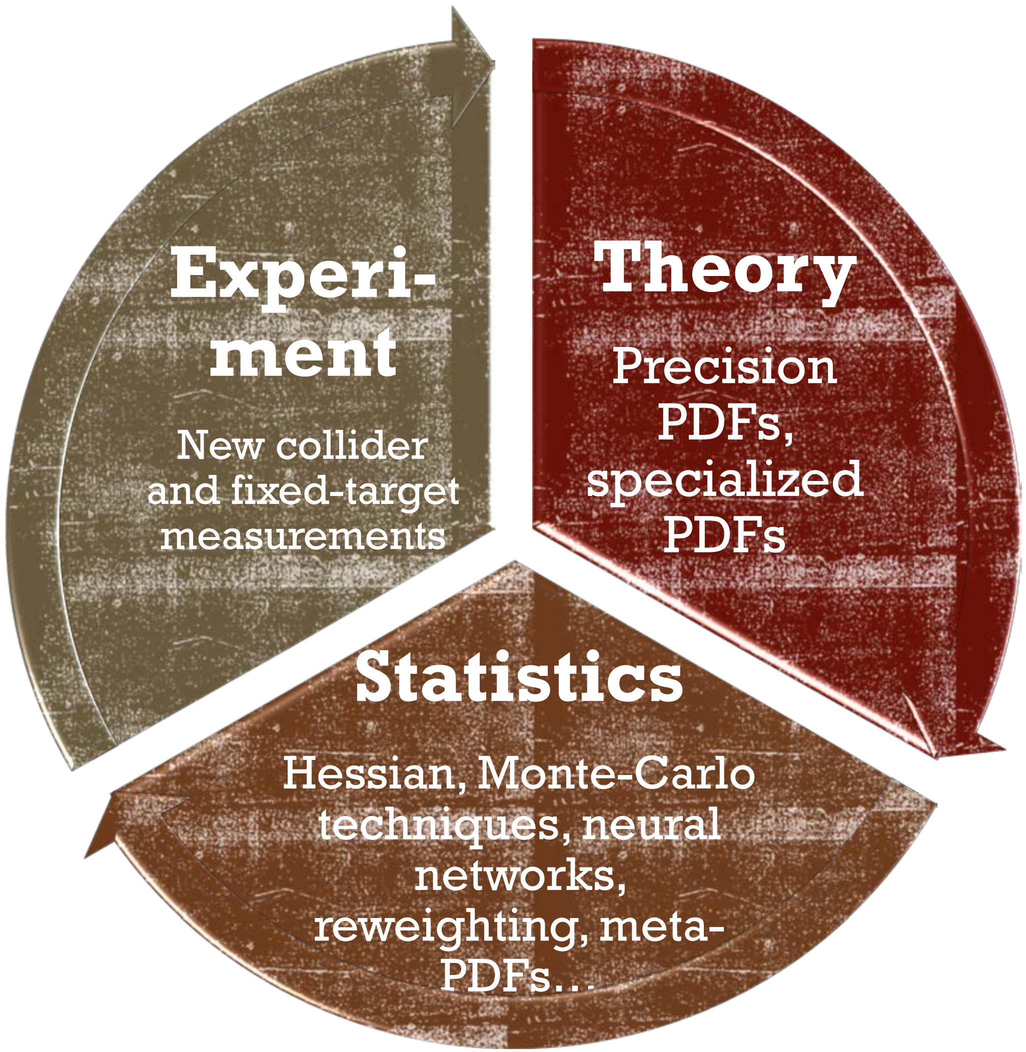

1. General-purpose NNLO PDFs

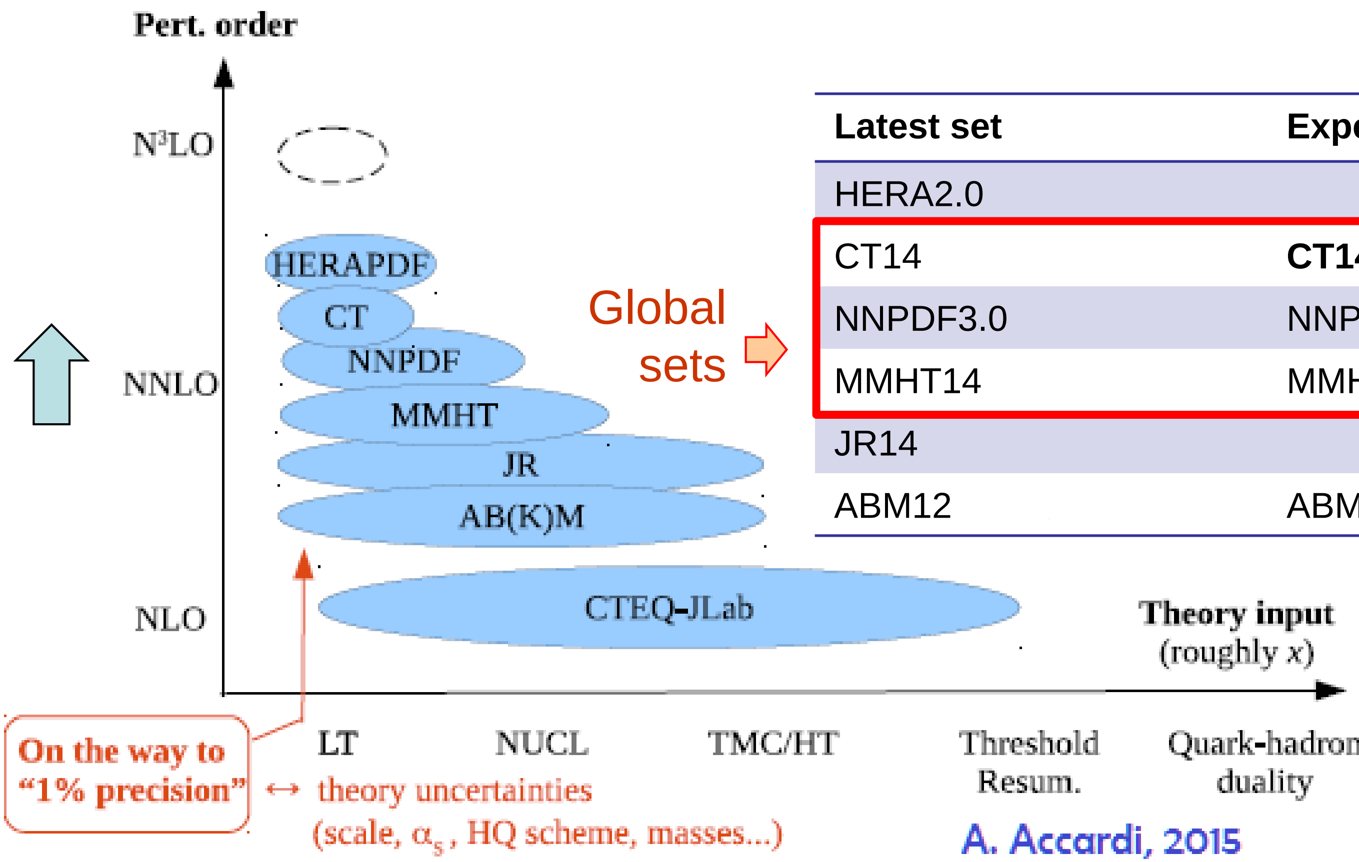

Latest set	Expected updates
HERA2.0	
CT14	**CT14HERA2**
NNPDF3.0	NNPDF3.1
MMHT14	MMHT+HERA2
JR14	
ABM12	ABMP16

2016 updates include new combined HERA1+2 data and 8 TeV LHC data

Expect mild changes in the PDFs and uncertainties

Map of experiments as a function of x and Q

For nucleon PDFs, experimental measurements are selected so as to reduce dependence on theoretical input beyond the leading power in perturbative QCD

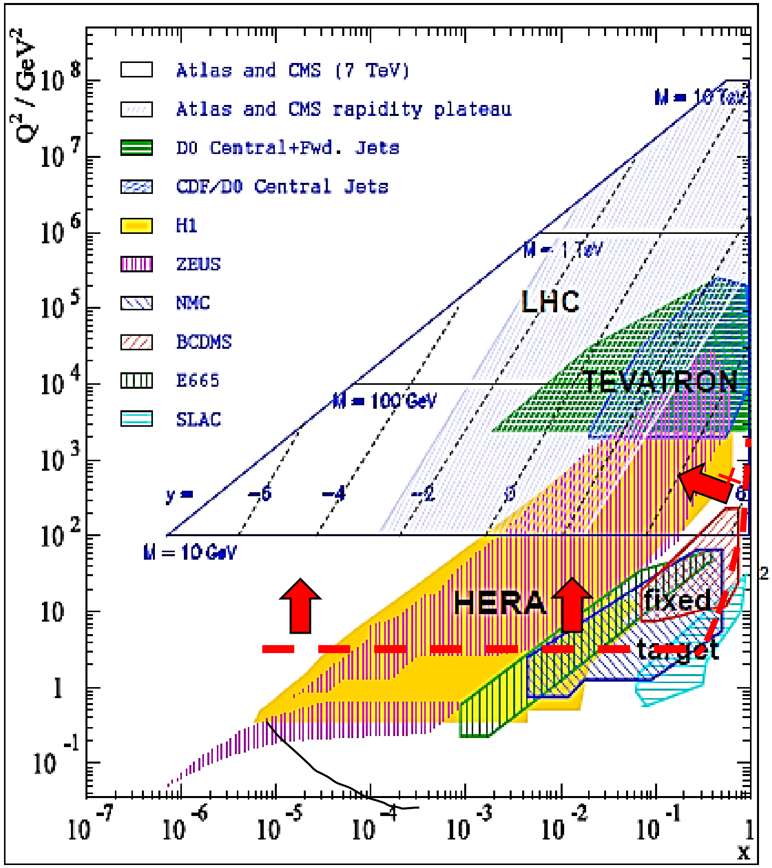

CT14:

only DIS data with $Q^2 > 4\ GeV^2$, $W^2 > 12.25\ \ GeV^2$ (above the red line) are accepted to ensure stable perturbative predictions

Include LHC W asymmetry and jet production data

Still using data from DIS and DY on **nuclear targets. CT14H2** does not use NMC DIS **on deuteron,** will be replaced by comparable future LHC/Tevatron measurements on **the proton**

Experiments in the CT14 analysis

33 **experiments**; χ^2/N_{pt} = 3252/2947 =1.10

Red arrows indicate new data sets

Experimental data set		N_{pt}	χ^2_e/N_{pt}
BCDMS F_2^p	[illegible]	[illegible]	[illegible]
BCDMS F_2^d	[illegible]	[illegible]	[illegible]
NMC F_2^d/F_2^p	[14]	123	1.08
NMC σ^p_{red}	[14]	201	1.85
CDHSW F_2^p	[15]	85	0.85
CDHSW F_3^p	[15]	96	0.83
CCFR F_2^p	[16]	69	1.02
CCFR xF_3^p	[17]	86	0.36
NuTeV $\nu\mu\mu$ SIDIS	[18]	38	0.62
NuTeV $\bar{\nu}\mu\mu$ SIDIS	[18]	33	1.18
CCFR $\nu\mu\mu$ SIDIS	[19]	40	0.72
CCFR $\bar{\nu}\mu\mu$ SIDIS	[19]	38	0.53
H1 σ_r^b	[20]	10	0.68
HERA charm production	[illegible]	47	1.26
HERA1 Combined NC and CC DIS	[22]	579	1.02
H1 F_L	[23]	9	1.92

Experimental data set		N_{pt}	χ^2_e/N_{pt}
[illegible] Drell-Yan process	[24]	119	0.98
[illegible]	[25]	15	0.87
E866 Drell-Yan process	[25]	184	1.37
CDF Run-1 electron A_{ch}	[26]	11	0.81
CDF Run-2 electron A_{ch}	[27]	11	1.24
D0 Run-2 muon A_{ch}	[29]	9	0.92
LHCb 7 TeV 35 pb^{-1} W/Z $d\sigma/dy_\ell$	[illegible]	14	0.7
LHCb 7 TeV 35 pb^{-1} A_{ch}, $p_{T\ell} > 20$ GeV	[illegible]	5	1.19
D0 Run 2 Z rapidity	[32]	28	0.59
CDF Run 2 Z rapidity	[33]	29	1.64
CMS 7 TeV 4.7 fb^{-1}, muon A_{ch}	[illegible]	11	0.8
CMS 7 TeV 840 pb^{-1}, electron A_{ch}	[illegible]	11	0.87
ATLAS 7 TeV 35 pb^{-1} W/Z cross sections and [illegible]	[illegible]	41	1.11
D0 Run-2 electron A_{ch} $(9.7 fb^{-1})$	[illegible]	13	1.79
CDF Run-2 inclusive jet production	[40]	72	1.45
D0 Run-2 inclusive jet production	[41]	110	1.09
ATLAS 7 TeV 35 pb^{-1} incl. jet production	[illegible]	90	0.55
CMS 7 TeV 5 fb^{-1} incl. jet production	[illegible]	133	1.33

CT10 NNLO PDFs do not include LHC data, but **predict** LHC Run-1 observables well

LHC 7 TeV data vs CT10 NNLO PDFs

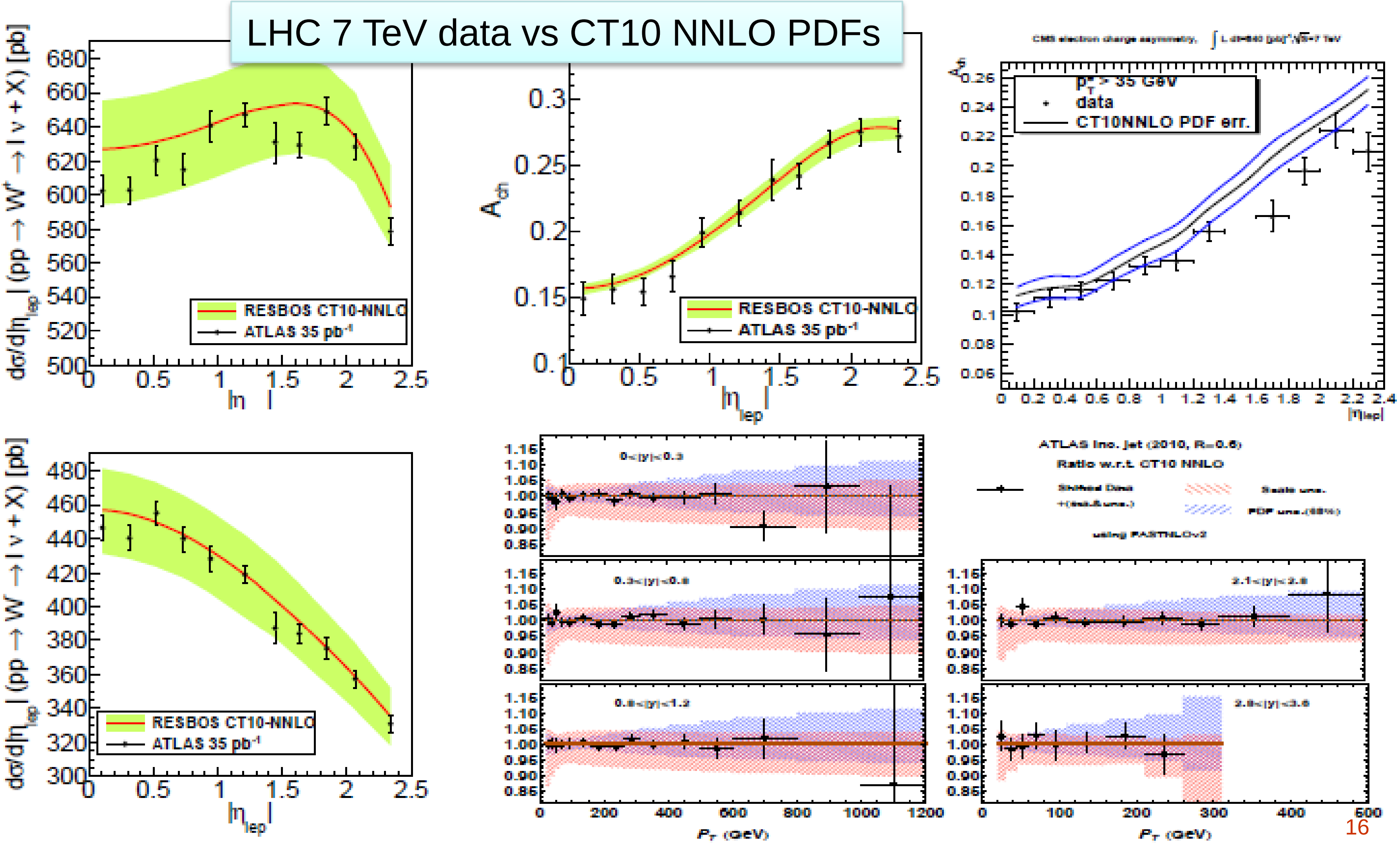

The ratios of W^+ to W^- and $(W^+ + W^-)$ to Z cross sections CT14HERA2 vs. CT14

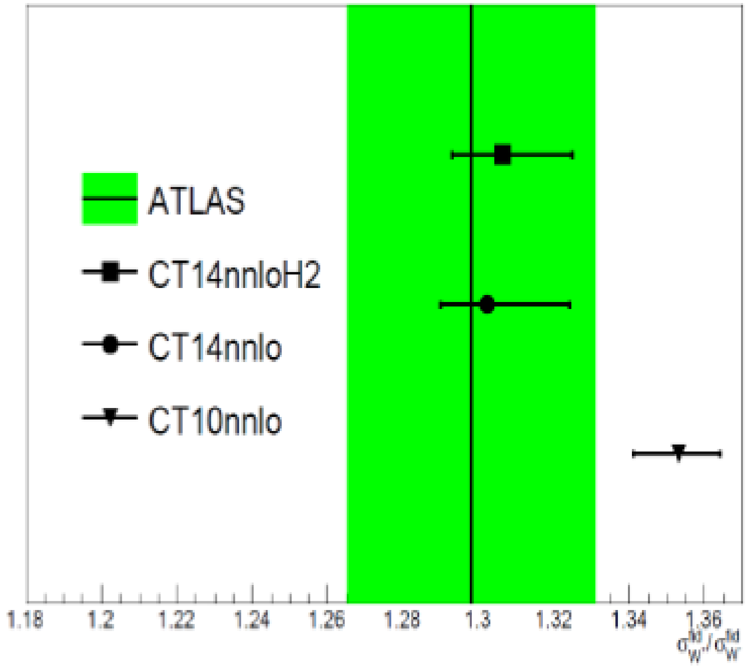

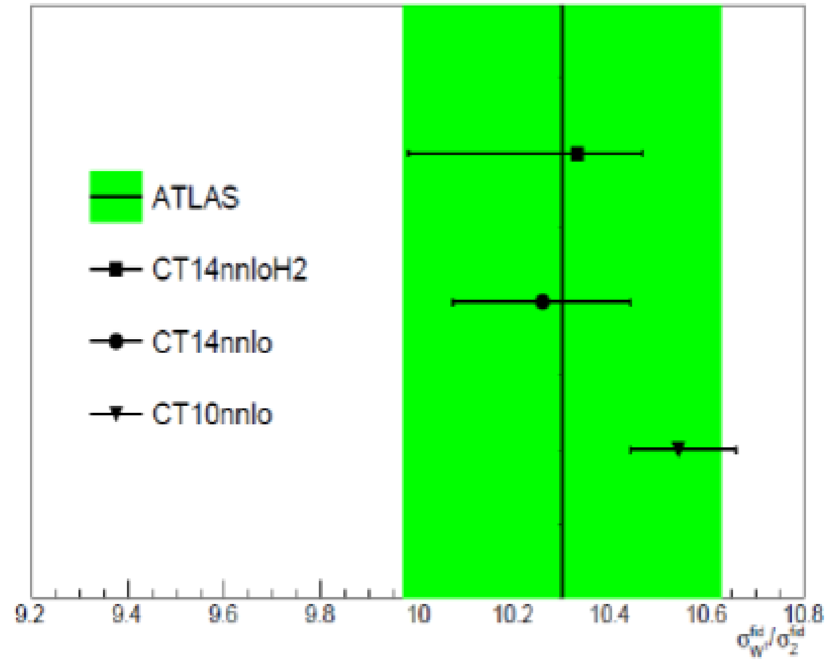

$$p_T^l > 25\ GeV\ , \quad |\eta_l| < 2.5\ , \quad 66 < m_{ll} < 116\ GeV$$

$$p_T^l > 25\ GeV\ , \quad p_T^\nu > 25\ GeV\ , \quad |\eta_l| < 2.5\ , \quad m_T > 50\ GeV$$

A rare exception

Compare CT14 and CT10 quark PDFs

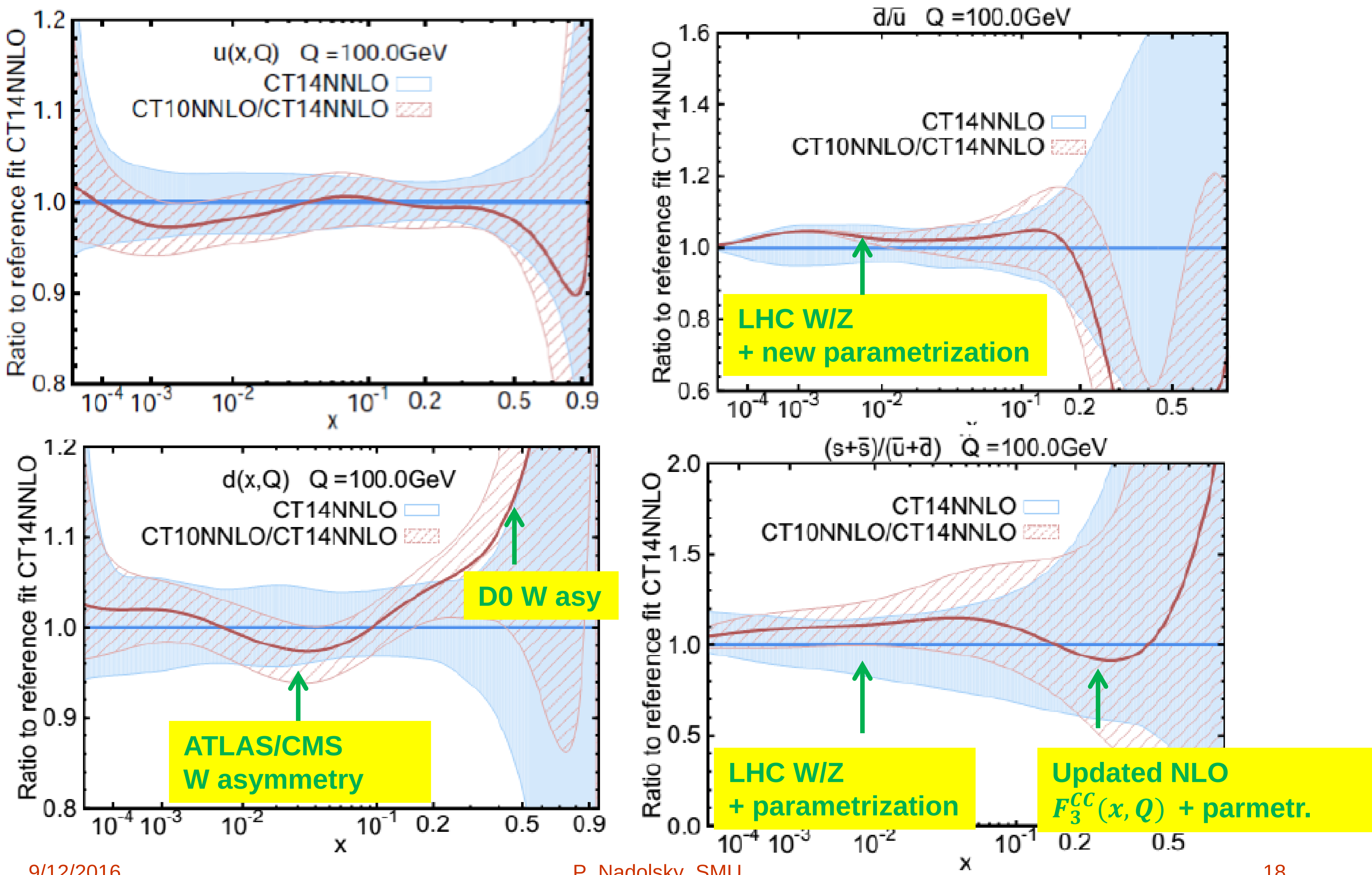

CT14 vs. CT10: the gluon PDF

$g(x, Q)$ is slightly higher in CT14 at $x \sim 0.05$ because of several effects.

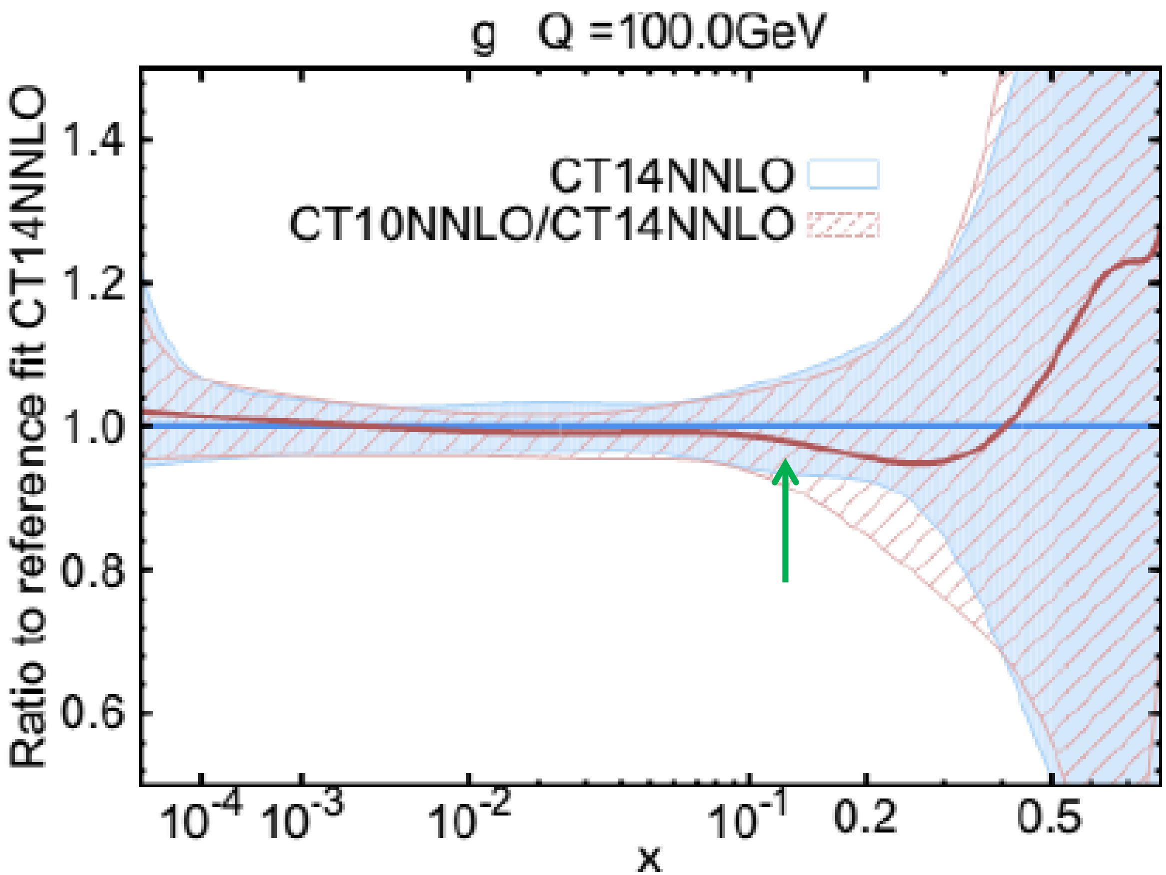

CT14 Higgs cross sections increase compared to CT10 by about 1-2%

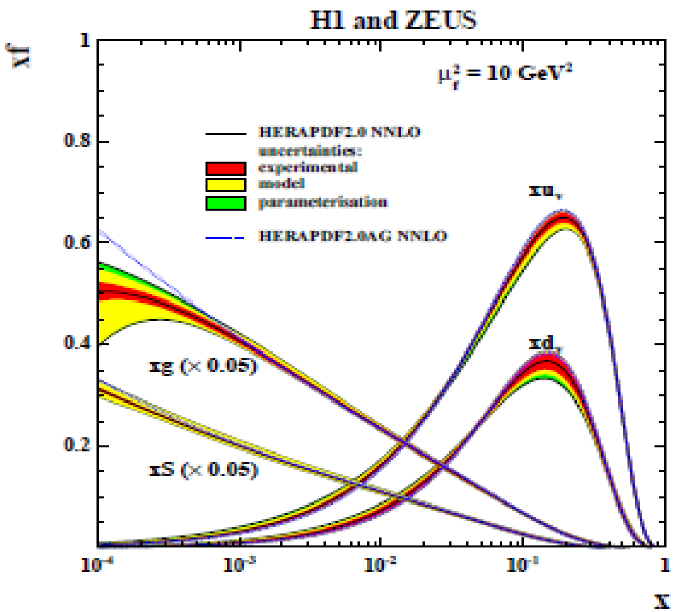

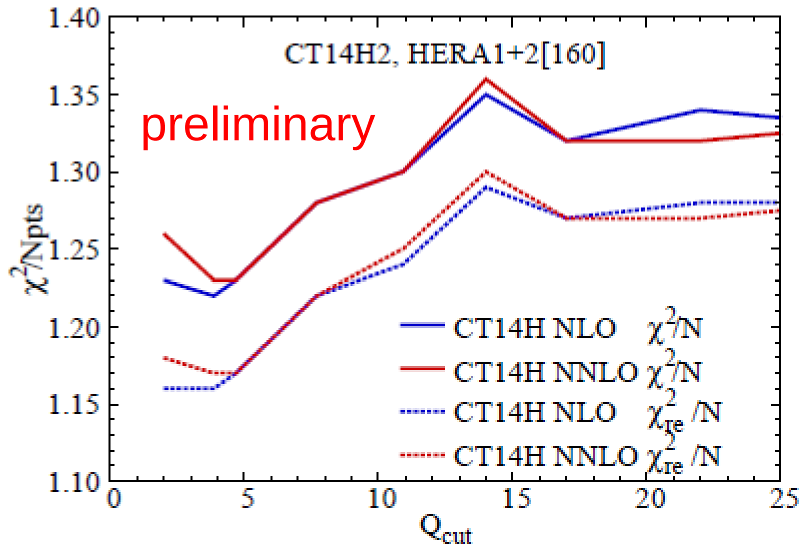

χ^2/N_{pts} with (top) and without (bottom) penalty for syst. shifts

The combined HERA1+2 data are included in HERA2.0, **CT14HERA2**, MMHT, and NNPDF3.1 analyses

$\chi^2/d.o.f. \sim 1.2$ for HERA1+2 tends to be elevated across all analyses, compared to $\chi^2/d.o.f. < 1.1$ for combined HERA1 data

$\Rightarrow$ This tension may arise from several sources

- Higher-twist corrections to $F_L(x,Q)$
- Small-x/saturation
- Experimental systematics (?)

The impact on global PDFs is mild, changes in PDFs do not exceed uncertainties

CT14HERA2 vs. CT14 at NNLO

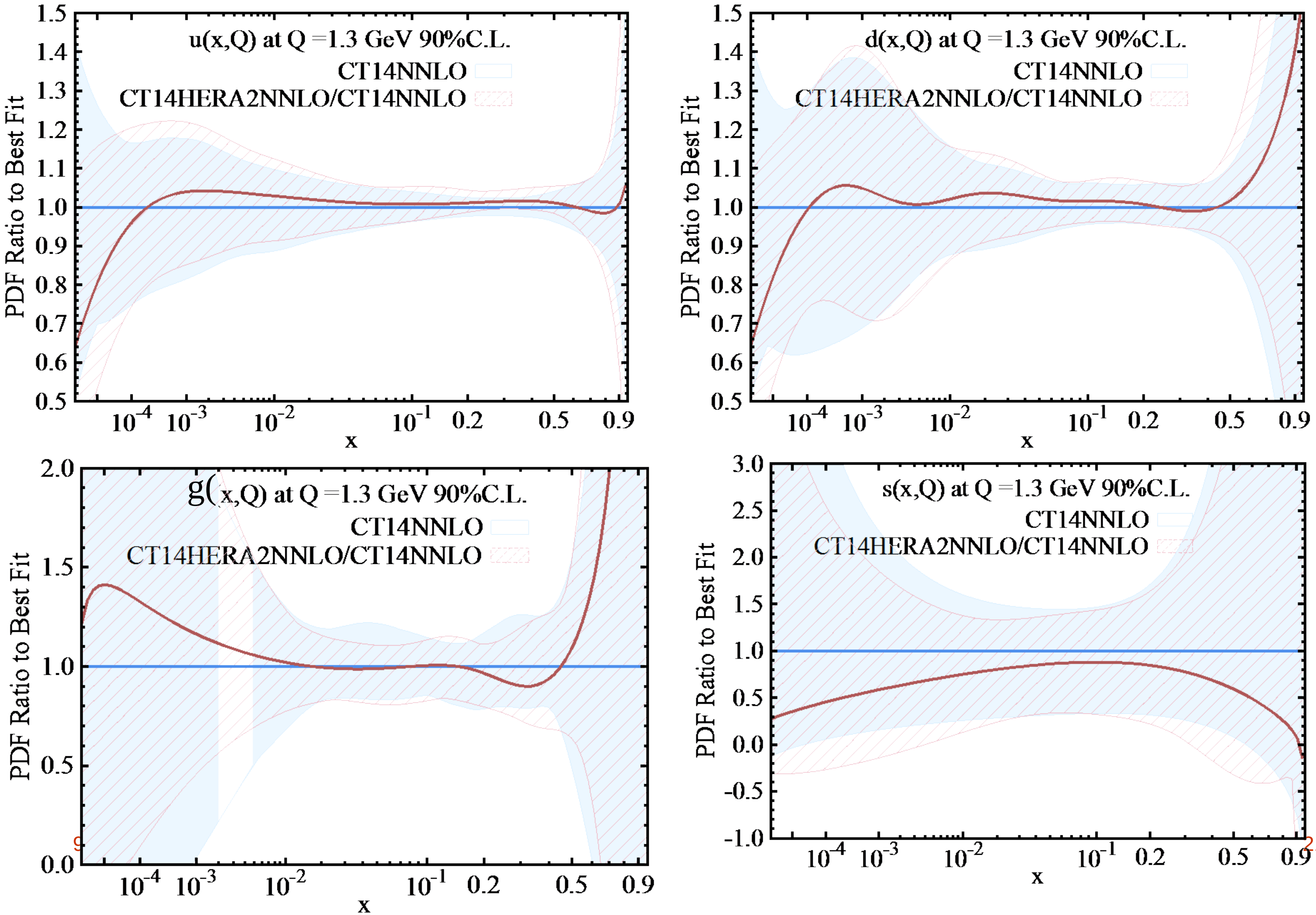

2. Specialized PDFs at NLO and NNLO

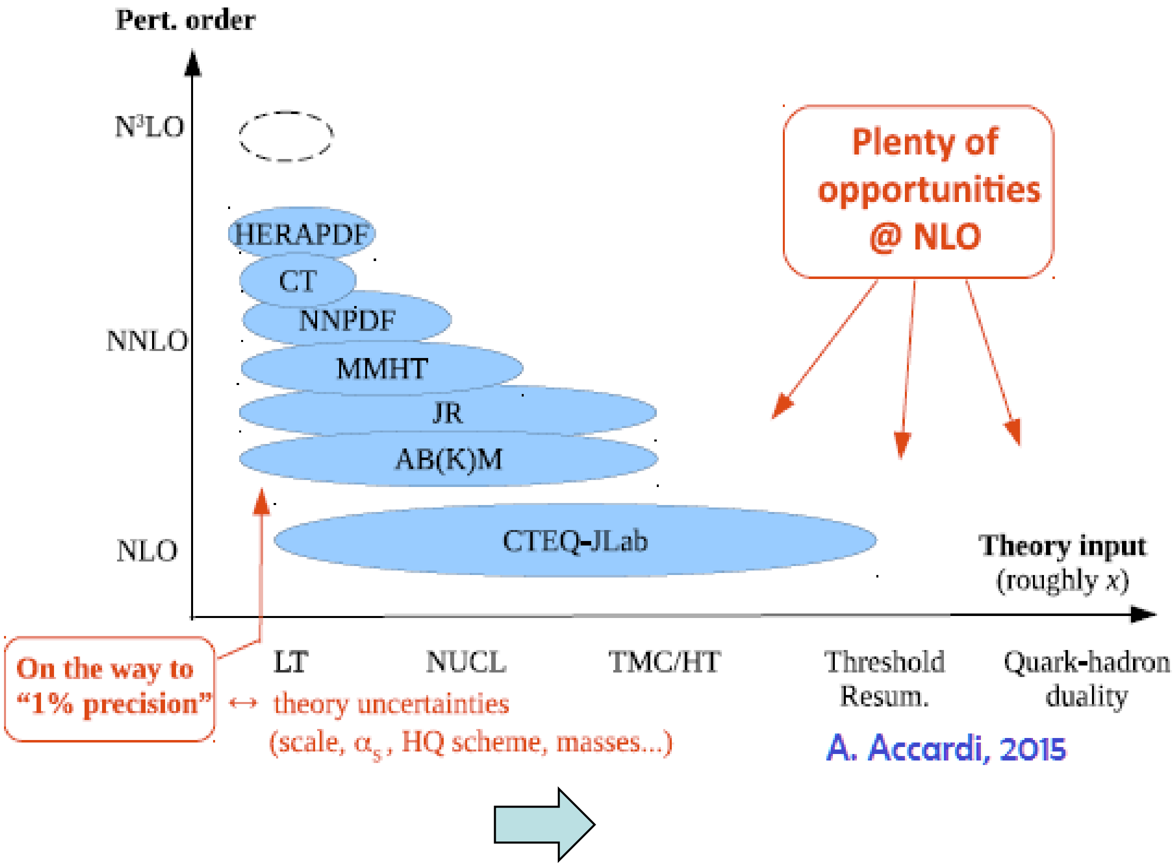

Are obtained under special assumptions or for special goals. May or may not be suitable for general physics

1. **CJ15:** NLO PDFs with large-x/low Q DIS data
2. **Most groups:** PDFs with up to 3, 4, 6 active flavors
3. **CT, NNPDF, MSTW:** QCD+QED PDFs
4. **CT, NNPDF:** PDFs with intrinsic charm
5. **NNPDF:** PDFs for threshold resummation
6. …

Photon PDFs

- Still in exploratory stage – limited experimental constraints, further theory developments needed (full NNLO QCD+(N)LO EM DGLAP evolution code, consistent EW corrections to all fitted cross sections)
- $u^p(x,Q) \neq d^n(x,Q)$ -- need more data to resolve difference
- **MRST QED** PDFs (hep-ph/0411040) : $f_\gamma^p(x,Q_0)$ is constructed from $u_v^p(x,Q_0)$, $d_v^p(x,Q_0)$, $P_{\gamma\leftarrow q}(x)$
- **NNPDF2.3 QED** (1308.0598): NN parametrization for $f_\gamma^p(x,Q_0)$, sequential QCD+QED evolution
- **CT14 QED** (1509.02905): generalized MRST $f_\gamma^p(x,Q_0)$, include $ep \to e\gamma X$ ZEUS data to constrain $f_\gamma^p(x,Q_0)$
- **CT14QEDinc** PDFs (new): photon PDFs with the elastic production component as the input condition at Q_0

CT14 QED PDFs

C. Schmidt, J. Pumplin, D. Stump, C.–P. Yuan, arXIv:1509.02905

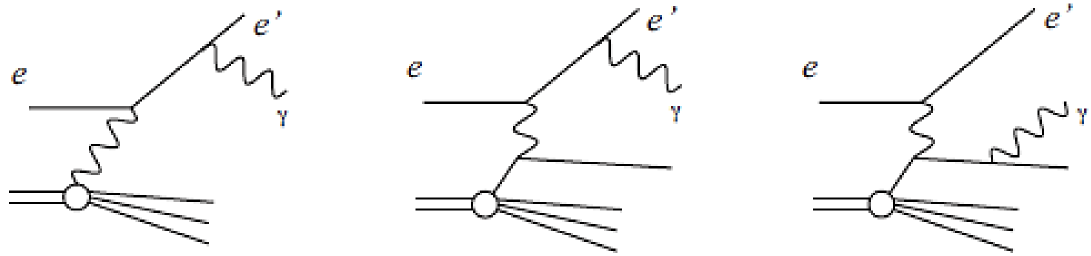

$|M|^2_{\gamma\gamma}$ $|M|^2_{LL}$ $|M|^2_{QQ}$ + interference

ZEUS $ep \to e\gamma X$ data ($N_{pt} = 8$) included to constrain $f_\gamma(x, Q)$

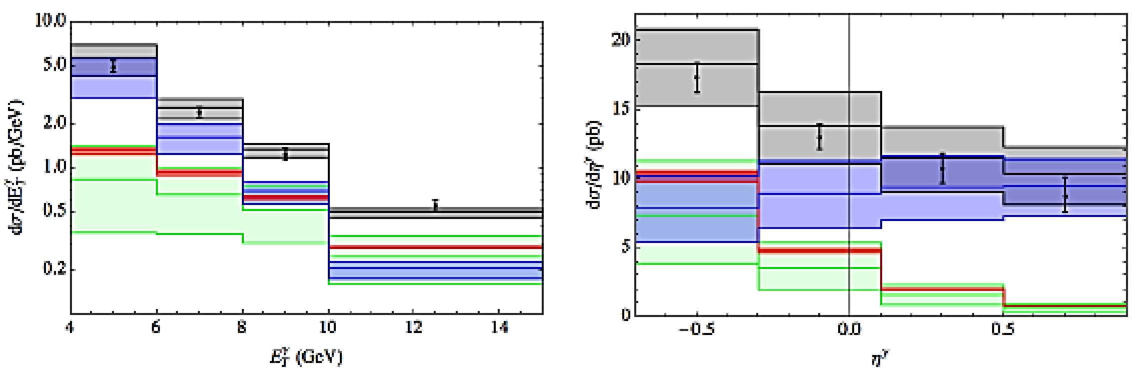

FIG. 4: Differential distributions for a zero initial photon PDF and using the smooth isolation prescription. The various bands display a variation in factorization scale between $0.5E_{\perp\gamma} \le \mu_F \le 2E_{\perp\gamma}$ and correspond to the total prediction (gray), the QQ component (blue), the LL component (red), and the photon-initiated contribution only (green).

Sharp cone and smooth cone photon isolations tried; rule out the "current-mass" radiative ansatz for $f_\gamma(x, Q_0)$ despite sizable theory uncertainties

CT14 QED PDFs

C. Schmidt, J. Pumplin, D. Stump, C.–P. Yuan, arXIv:1509.02905

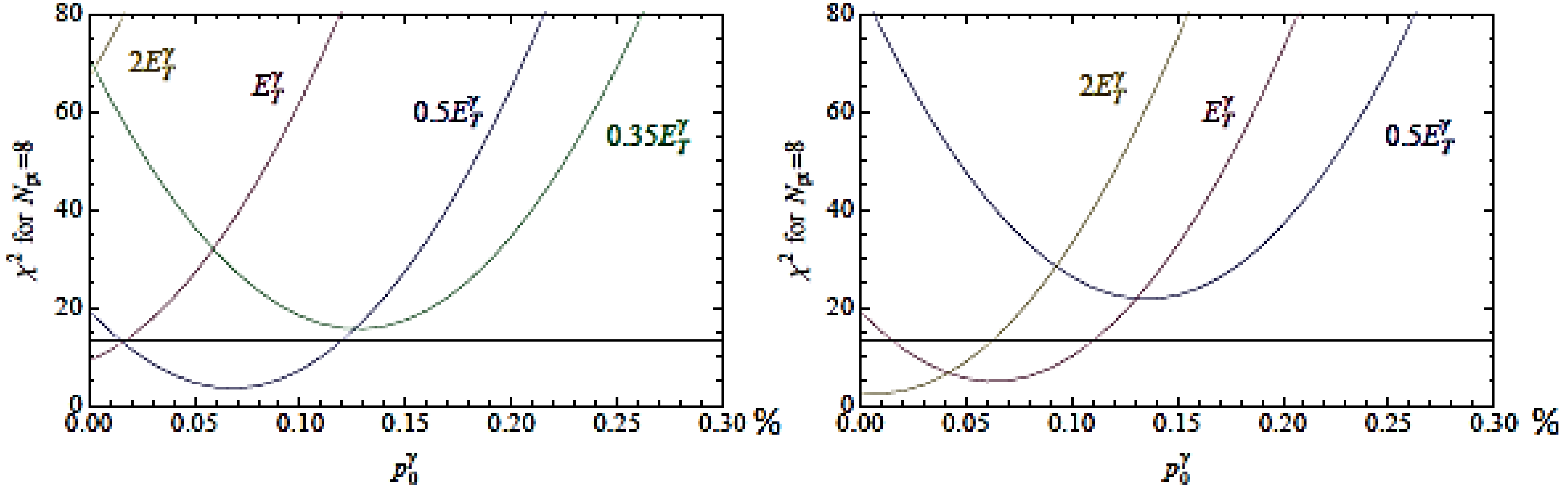

FIG. 9: Plots of χ^2 versus initial photon momentum fraction p_0^γ using the smooth isolation prescription (left) and the sharp isolation prescription (right) for factorization scales $\mu_F = 2E_{\perp\gamma}$, $E_{\perp\gamma}$, $0.5E_{\perp\gamma}$, and $0.35E_{\perp\gamma}$. The horizontal line at $\chi^2 = 13.36$ is the 90% confidence level limit for 8 data points.

Photon momentum fractions > 0.14% are disfavored, for the given isolation models

NLO photon PDFs at Q=3.2, 85, 1000 GeV

CT14QED with $p_0^\gamma = 0\%$ (green), CT14QED with $p_0^\gamma = 0.14\%$ (black), MRST2004QED0 using current quark masses (orange), MRST2004QED1 using constituent quark masses (brown), and NNPDF2.3QED with $\alpha_s = 0.118$ and average photon (blue).

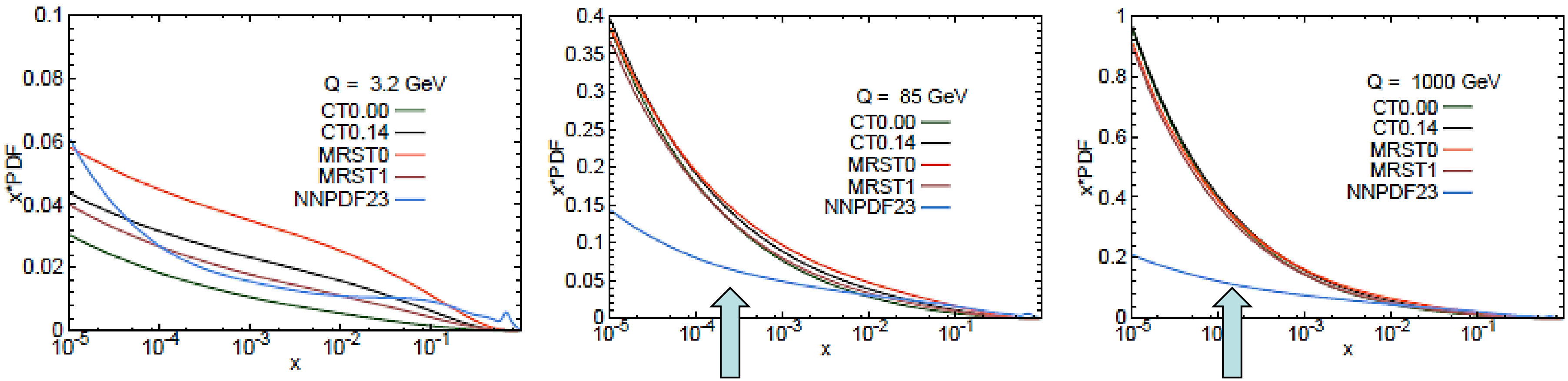

Slower DGLAP evolution of NNPD2.3 due to the factorized approximation for QCD+QED evolution operator ?

Uncertainty bands cover all central predictions

Photon-Photon Luminosity

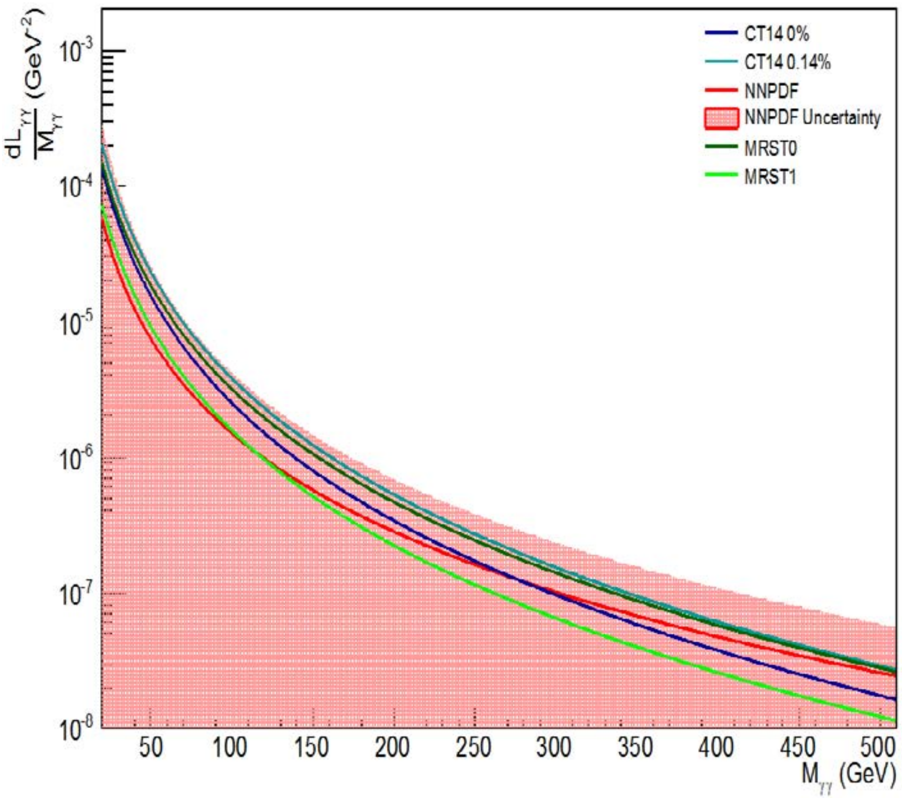

FIG. 4: Photon-photon luminosity for an invariant mass of 20 GeV to 500 GeV for 13 TeV collider energy

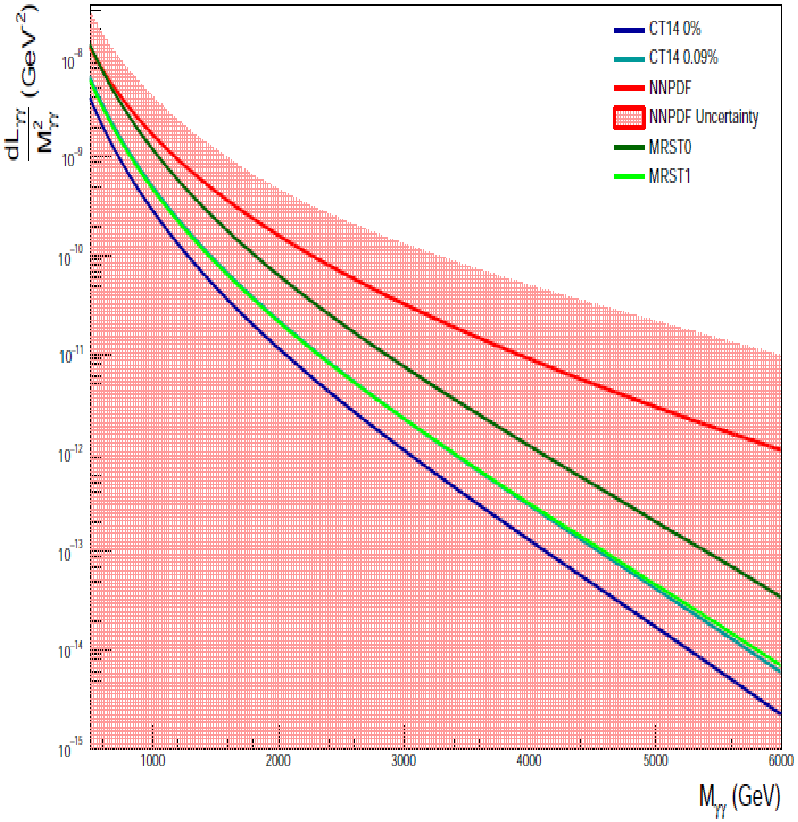

FIG. 5: Photon-photon luminosity for and invariant mass of 500 GeV to 6000 GeV for 13 TeV collider energy

- Central NNPDF photon harder at large x.

CT14QED Photon PDFs

- Important point:

$$\left(f_{\mathrm{EPA}}+f_{\mathrm{inelastic}}\right)(x,Q) \approx f_{\mathrm{EPA}}(x,Q)+f_{\mathrm{inelastic}}(x,Q)$$

- $f_{\mathrm{EPA}}(x,Q)$ changes little from Q_0 to Q because of falloff from form factor
- Up to corrections of order α, the photon PDF evolves additively:

$$f(x,Q) \approx f(x,Q_0)+\int_{Q_0^2}^{Q^2}\frac{dQ^2}{Q^2}\frac{\alpha}{2\pi}P_{\gamma q}\circ\sum e_q^2 f_q(x,Q)$$

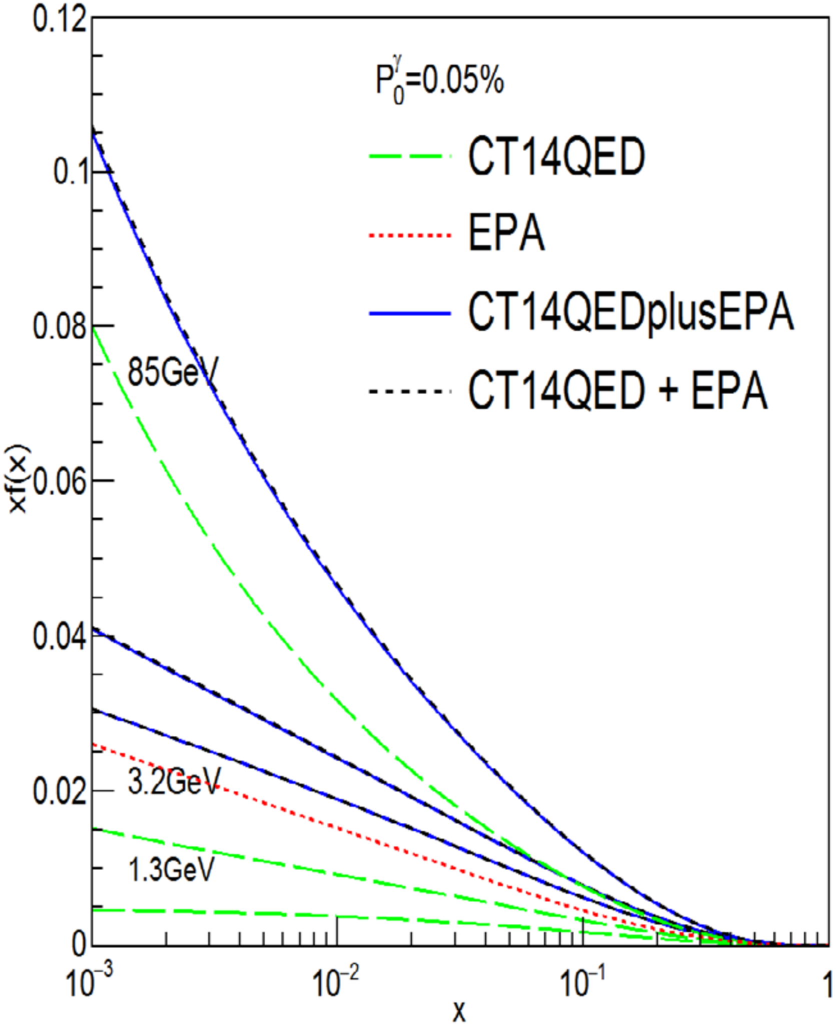

- The measured cross-sections are compared to theoretical predictions using a selection of recent PDFs.
- Theory uncertainties are larger than measurement uncertainties => potential for PDF constraints.
- Photon induced contribution reaches 15%.

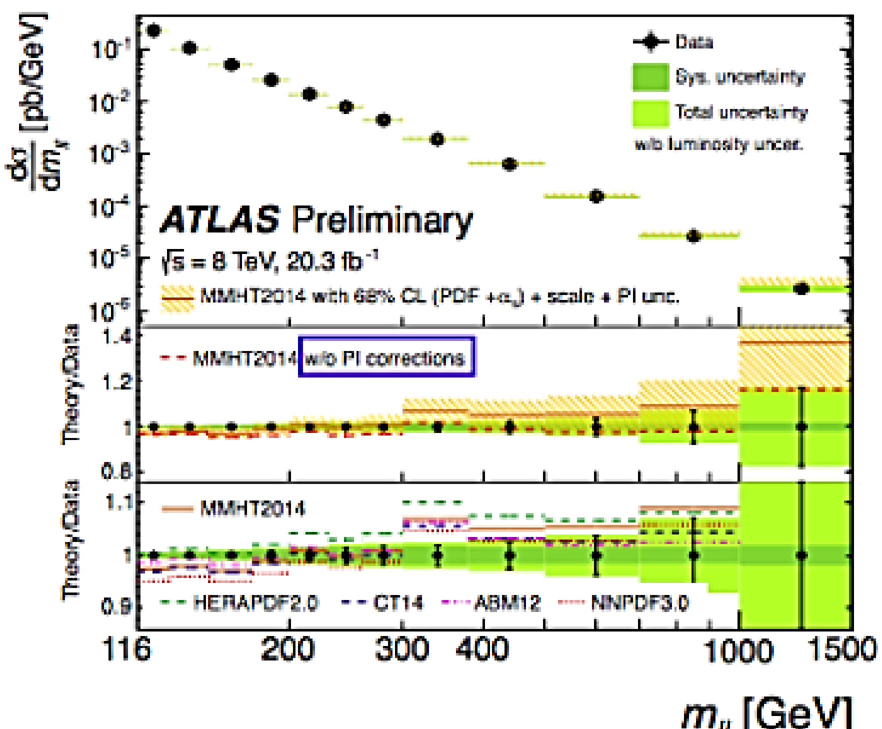

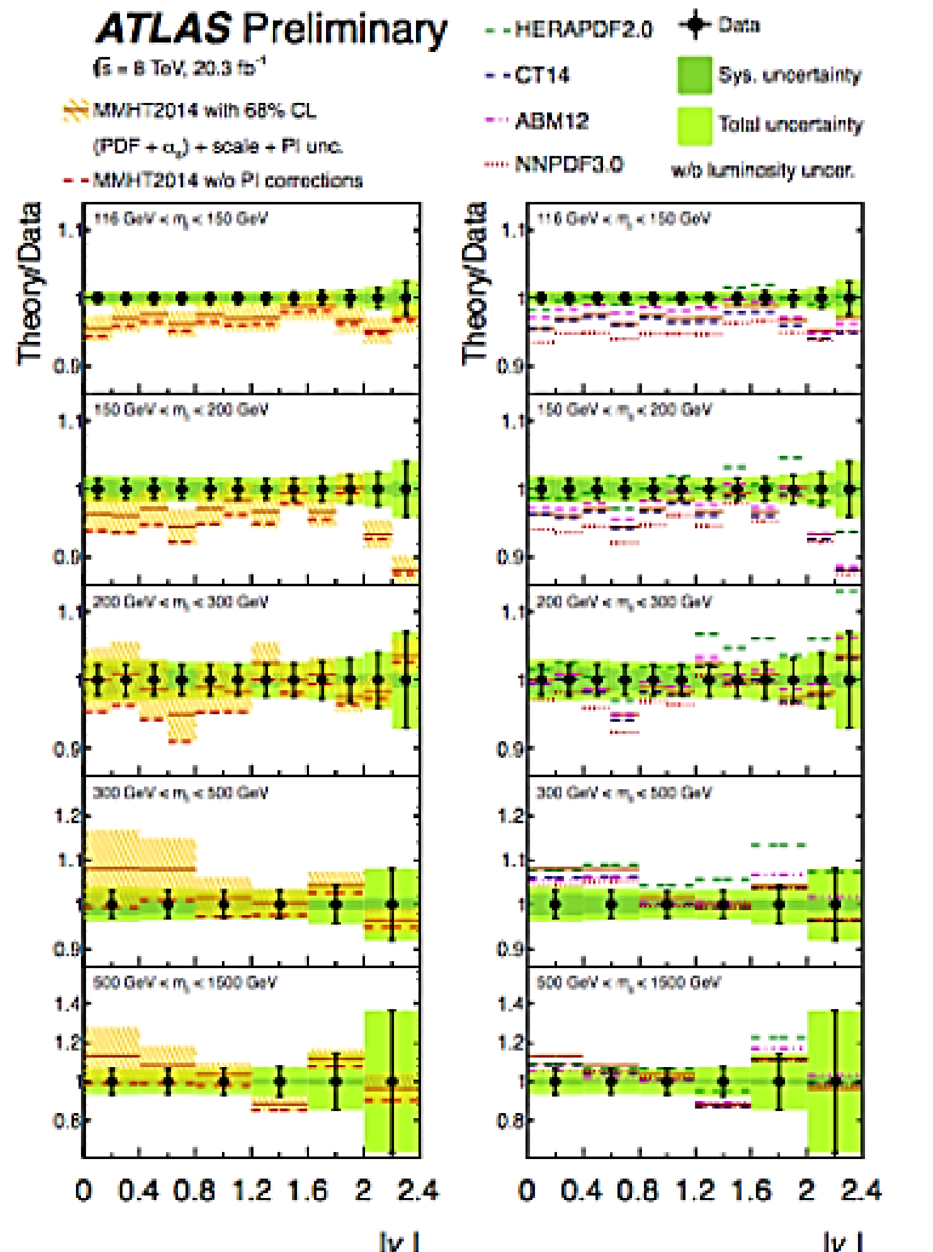

Compare CMS Data to various photon PDFs

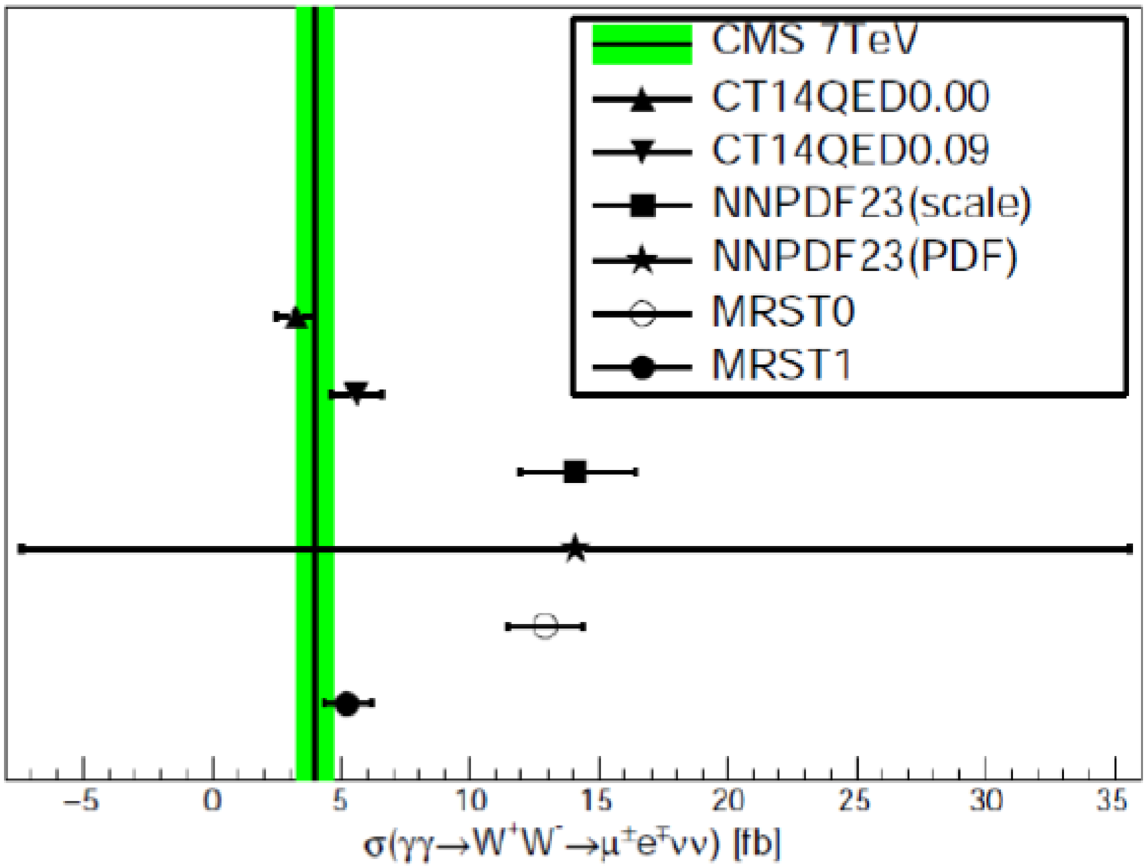

CT14 Monte-Carlo replicas with positivity and asymmetric standard deviations (T. J. Hou et al., arXiv:1607.06066)

Generalized method to convert Hessian PDFs into Monte-Carlo replicas while reproducing asymmetric uncertainties and positivity of individual PDF sets

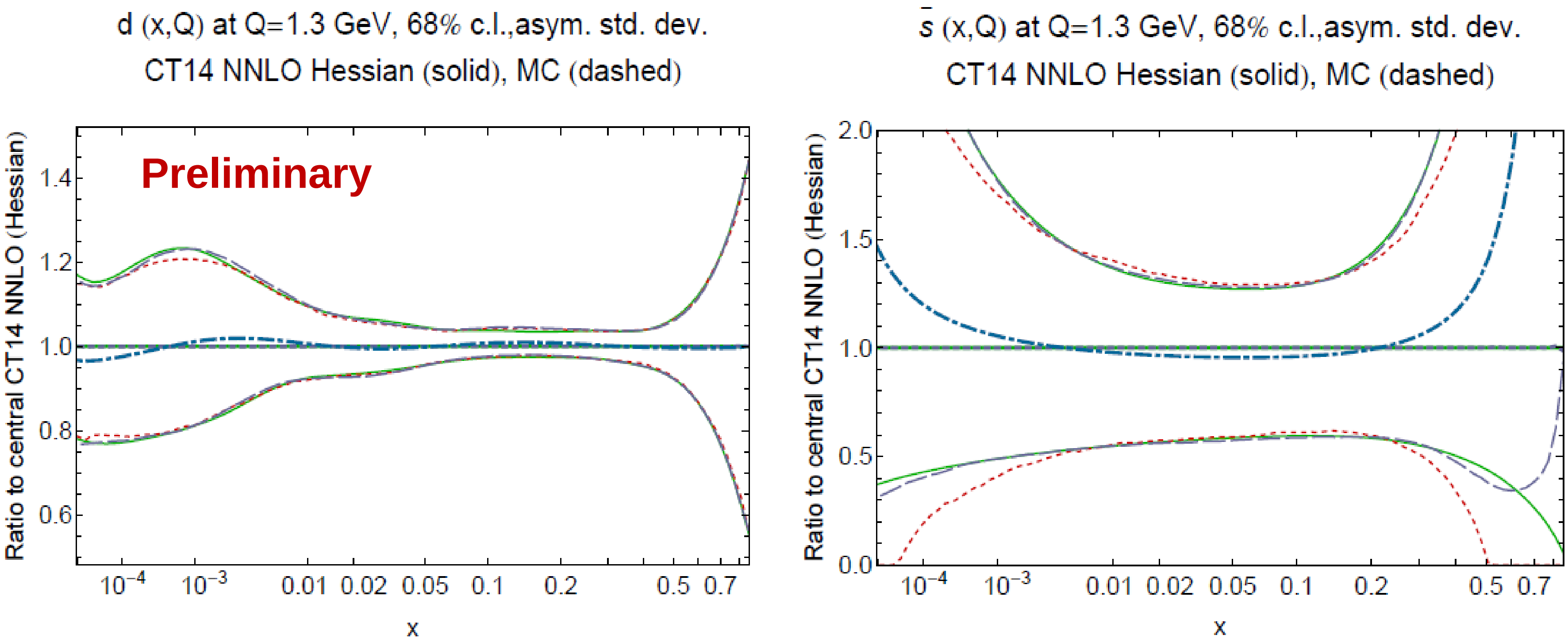

Green: Hessian std. deviation

Red: Symmetric MC std. dev.

Thin blue: Asymmetric MC std. dev.

Thick blue: Asymmetric MC median

Good agreement between green and light blue in central regions, smooth behavior

Estimating the PDF+α_s uncertainty in practical applications

OUTP-15-17P
SMU-HEP-15-12
TIF-UNIMI-2015-14
LCTS/2015-27

PDF4LHC recommendations for LHC Run II

Jon Butterworth[1], Stefano Carrazza[2], Amanda Cooper-Sarkar[3], Albert De Roeck[4,5], Joël Feltesse[6], Stefano Forte[2], Jun Gao[7], Sasha Glazov[8], Joey Huston[9], Zahari Kassabov[2,10], Ronan McNulty[11], Andreas Morsch[4], Pavel Nadolsky[12], Voica Radescu[13], Juan Rojo[14] and Robert Thorne[1].

Read for detailed suggestions on selecting and using PDFs in various situations

A major revision of the previous PDF4LHC recommendation in arxiv:1101.0538, arXiv:1211.5142

+ 2 follow-up contributions in 2015 Les Houches proceedings

The Battle Royal

PDF4LHC recommendations
for LHC Run-II
(arXIV:1510.03865)

Recommendations for
PDF usage in LHC
predictions
(arXIV:1603.08906)

WHOSE LAW WILL PREVAIL?

Given numerous PDF sets, what is the PDF uncertainty in my analysis?

$pp \to t\bar{t}X$

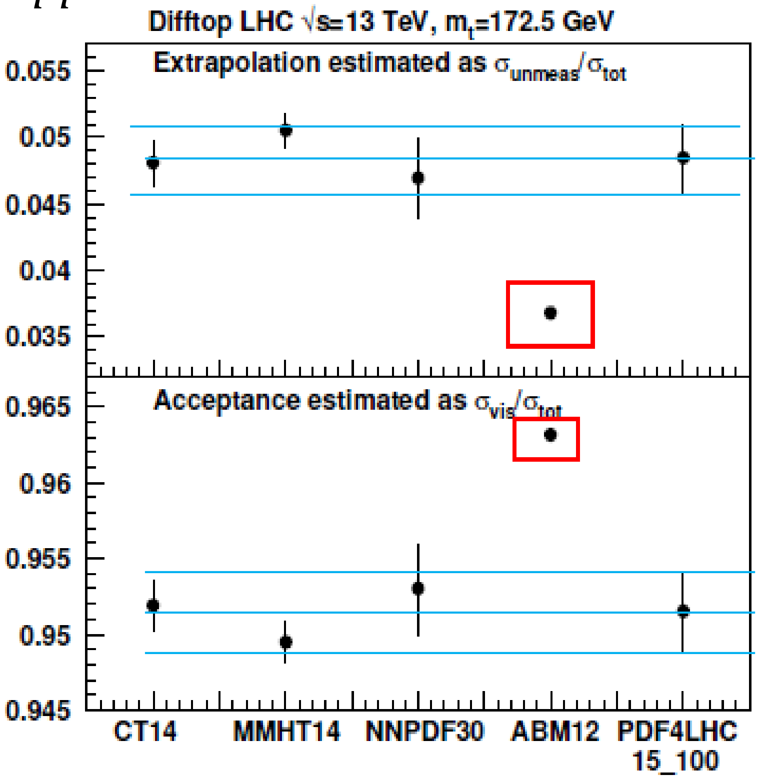

Figure: K. Lipka
1603.08906

The procedure for computing the PDF uncertainty must vary depending on the goals. The options may include

a) Using one individual set out of several similar ones (e.g., CT, MMHT, or NNPDF)

b) Using an envelope of all sets, including the outlier sets

Why PDF4LHC recommendation is necessary

Estimates of PDF uncertainties may vary drastically depending on the method.

An overly conservative estimate greatly reduces sensitivity to BSM physics.

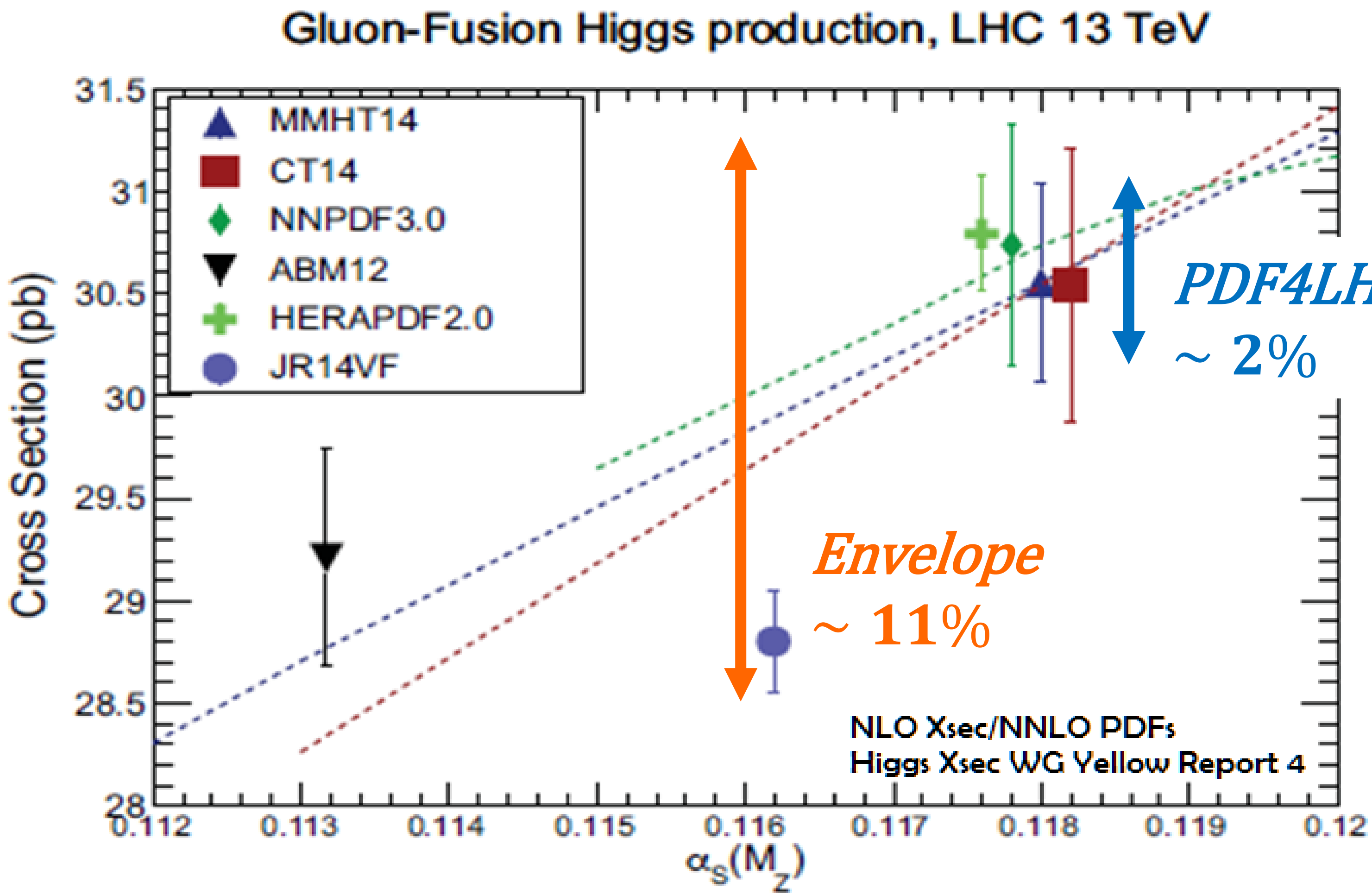

Why PDF4LHC recommendation is needed

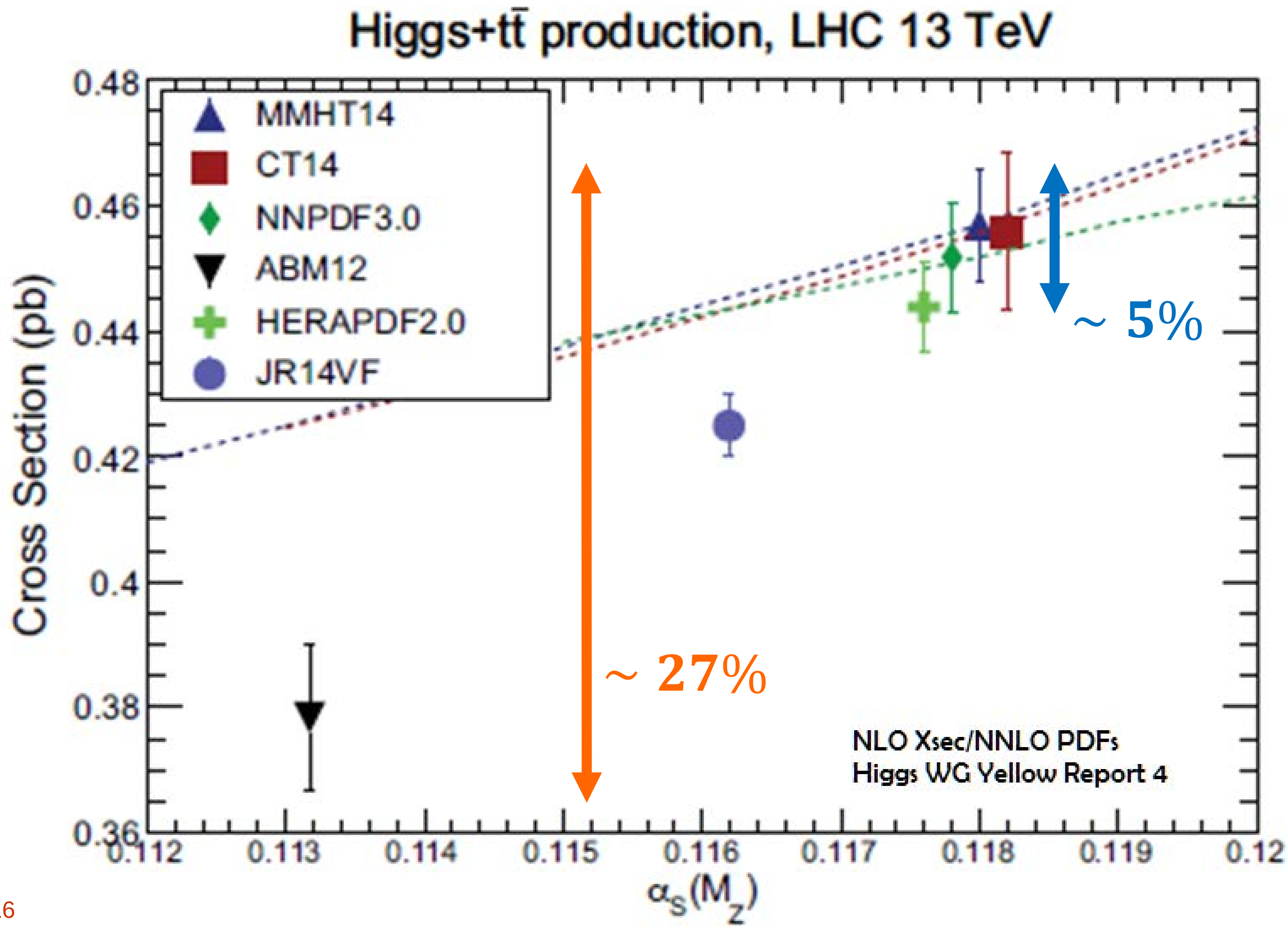

PDF4LHC publication, topics

1. **Review of updates on PDFs from various groups**

NNLO Global PDF sets: CT14, MMHT'14, NNPDF3

PDFs using other methodologies: ABM'12, CJ15, HERAPDF2.0

2. Average PDF sets by PDF4LHC group: PDF4LHC15_30, _100, _MC

Criteria for combination

$\alpha_s(M_Z) = 0.1180 \pm 0.0015$ at 68% c.l.

3. Recommendation on selecting PDF sets for various LHC applications

A. New physics searches

B. Precision tests of SM and PDFs

C. Monte-Carlo simulations

D. Acceptance estimates

Average PDF sets **can** be used **for bulk of applications** in A, C, D

Now on LHAPDF:

NLO, NNLO, varied α_s sets
$N_f = 5$ and 4 (upcoming)

LHAPDF6 grid	Pert order	ErrorType	N_{mem}	$\alpha_s(m_Z^2)$
PDF4LHC15_nnlo_mc	NNLO	replicas	100	0.118
PDF4LHC15_nnlo_100	NNLO	symmhessian	100	0.118
PDF4LHC15_nnlo_30	NNLO	symmhessian	30	0.118
PDF4LHC15_nnlo_mc_pdfas	NNLO	replicas+as	102	mem 0:100 $\to$ 0.118 mem 101 $\to$ 0.1165 mem 102 $\to$ 0.1195
PDF4LHC15_nnlo_100_pdfas	NNLO	symmhessian+as	102	mem 0:100 $\to$ 0.118 mem 101 $\to$ 0.1165 mem 102 $\to$ 0.1195
PDF4LHC15_nnlo_30_pdfas	NNLO	symmhessian+as	32	mem 0:30 $\to$ 0.118 mem 31 $\to$ 0.1165 mem 32 $\to$ 0.1195
PDF4LHC15_nnlo_asvar	NNLO	-	1	mem 0 $\to$ 0.1165 mem 1 $\to$ 0.1195

Table 5: Summary of the combined NNLO PDF4LHC15 sets with $n_f^{\max} = 5$ that are available from LHAPDF6. The corresponding NLO sets are also available. Members 0 and 1 of PDF4LHC15_nnlo_asvar coincide with members 101 and 102 (31 and 32) of PDF4LHC15_nnlo_mc_pdfas and PDF4LHC15_nnlo_100_pdfas (PDF4LHC15_nnlo_30_pdfas). Recall that in LHAPDF6 there is always a zeroth member, so that the total number of PDF members in a given set is always $N_{\text{mem}} + 1$. See text for more details.

Averaging of PDF ensembles

The 2012 recommendation estimated the combined uncertainty as an envelope of **cross sections** for 3 PDF sets; the envelope was overly sensitive to outliers

By 2015, several methods for combination (averaging) of **PDFs** (before computing cross sections) were developed. Criteria allowing the combination were outlined.

Combination workflow:

1. Generate 900 MC replicas from all input ensembles (currently CT14, MMHT14, NNPDF3.0) using Thorne-Watt procedure

   Other PDF sets can be added in the future if they satisfy the listed criteria

2. Reduce the number of final replicas from 900 to 100 or 30 by keeping most relevant PDF combinations

Reduced sets

- 900 error PDFs are too much for general use
- 3 reduction techniques have been developed
  - Compressed Monte Carlo PDFs (PDF4LHC15_nnlo(nlo)_mc)
    - 100 PDF error sets; preserve non-Gaussian errors
  - **META Hessian PDFs (PDF4LHC15_nnlo(nlo)_30**
    - 30 PDF error sets using METAPDF technique; Gaussian (symmetric) errors
  - MCH Hessian PDFs (PDF4lhc15_nnlo(nlo)_100
    - 100 PDF error sets using MCH technique; Gaussian (symmetric errors)
- The META technique is able to more efficiently reproduce the uncertainties when using a limited number (30) of error PDFs
- The MCH technique best reproduces the uncertainties of the 900 MC set prior

Comparisons of ensembles with 900, 100, 30 replicas

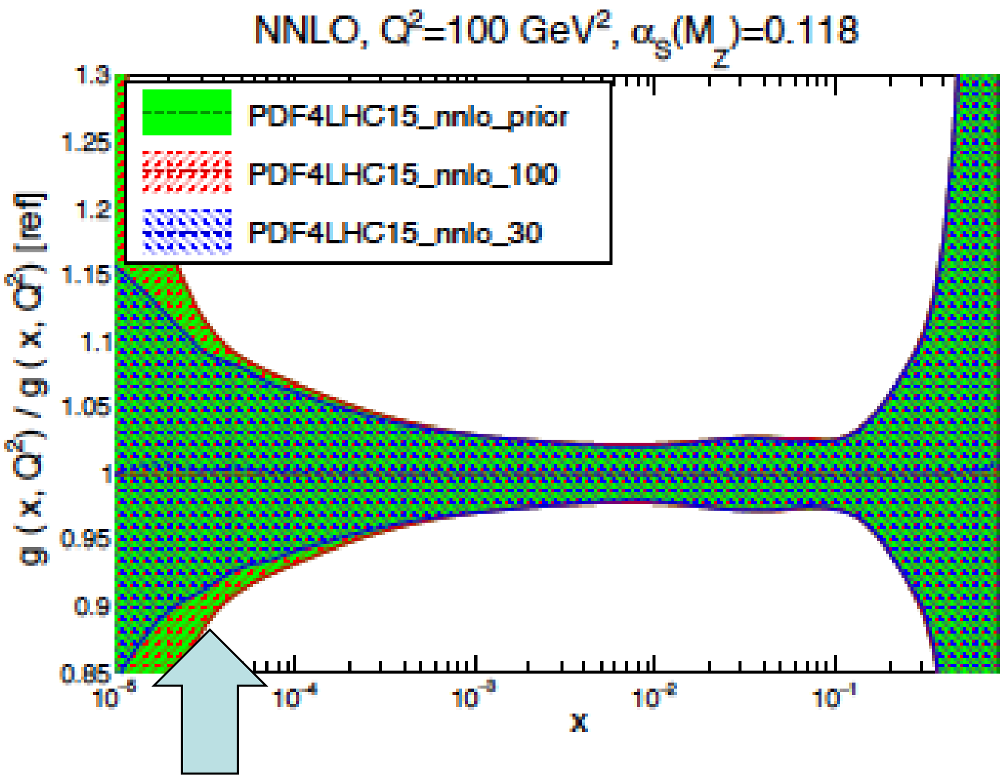

Three reduced PDF4LHC sets (100, MC, 30) reproduce well the 900-replica prior. Keep in mind that the uncertainty of the prior has an uncertainty of its own. By their construction, the lowest Hessian eigenvector sets are known the best, the highest sets are known with less confidence.

The 30-member ensemble keeps the lowest, best known sets and thus provides a lower estimate for the _900 prior uncertainty, known with higher confidence. When this estimate is not sufficient, or non-Gaussianities are important, use the 100 and MC sets

Ranges with differences between input PDFs, prior, and reduced sets

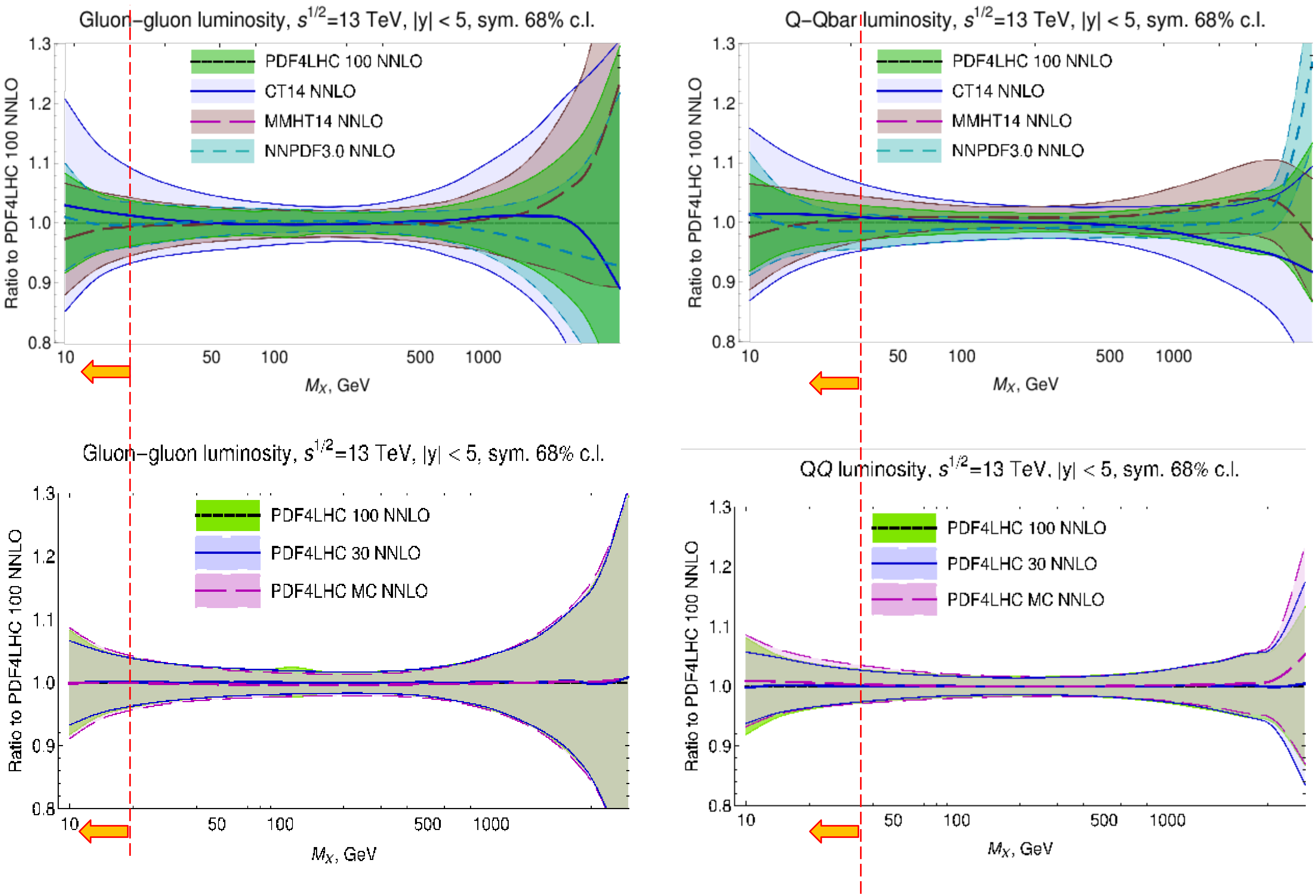

Note the $|y| < 5$ cut to constrain comparisons to the experimentally accessible region

Dependence of LHC observab...

metapdf.hepforge.org/2016_pdf4lhc/

Search

METAPDF is hosted by Hepforge, IPPP Durhan

Dependence of LHC observables on parton distribution functions

CONTENTS

1. $p + p \to Z + X$

   [settings of the calculation] [Applgrid files]
   - PDF4LHC15 PDFs (NLO)
   - PDF4LHC15 PDFs (NNLO)
   - PDF4LHC15_100, HERA, ABM PDFs (NNLO)
   - PDF4LHC15_100, CT14, MMTH14, NNPDF3.0 PDFs (NNLO)

2. $p + p \to W^+ + X$

   [settings of the calculation] [Applgrid files]
   - PDF4LHC15 PDFs (NLO)
   - PDF4LHC15 PDFs (NNLO)

META gallery for basic processes at 7, 8, 13 TeV

Developed by Bo Ting Wang and Keping Xie

$p + p \to W^+ + X$

[settings of the calculation] [Applgrid files]

PDF4LHC15 PDFs (NLO)

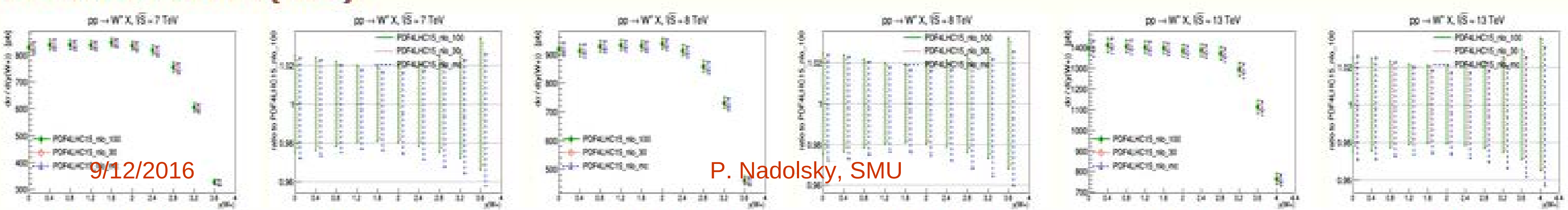

[pdf] [eps] [pdf] [eps] [pdf] [eps] [pdf] [eps] [pdf] [eps] [pdf] [eps]

Gallery of phenomenological comparisons for LHC

Process	Order	Type of calculation
•$p + p \rightarrow Z + X$	NLO	aMCFast/APPLgrid
•$p + p \rightarrow W^{+} + X$	NLO	aMCFast/APPLgrid
•$p + p \rightarrow W^{-} + X$	NLO	aMCFast/APPLgrid
•$p + p \rightarrow t\bar{t} + X$	NLO	aMCFast/APPLgrid
•$p + p \rightarrow t\bar{t} + X$	NLO	aMCFast/APPLgrid
•$p + p \rightarrow t\bar{t}\gamma\gamma + X$	NLO	aMCFast/APPLgrid
•ATLAS inclusive jets	NLO	NLOJET++/APPLgrid
•ATLAS inclusive dijets	NLO	NLOJET++/APPLgrid
•$P + p \rightarrow W^{+} c + X$	NLO	aMCFast/APPLgrid
•$P + p \rightarrow W^{-} c + X$	NLO	aMCFast/APPLgrid
•$P + p \rightarrow H + X$	LO,NLO	MCFM
•$P + p \rightarrow H +$ jet $+ X$	LO, NLO	MCFM

Compared PDFs: PDF4LHC15_100, _30, _MC, ABM'12, CT14, HERA2.0, MMHT14, NN3.0

Both full (MCFM) and fast (ApplGrid) calculations. AppGrlids are generated with minimal cuts and can be downloaded.

MCFM: compare PDF and Monte-Carlo integration errors

Differences of PDF4LHC PDFs matter only when MC errors are negligible

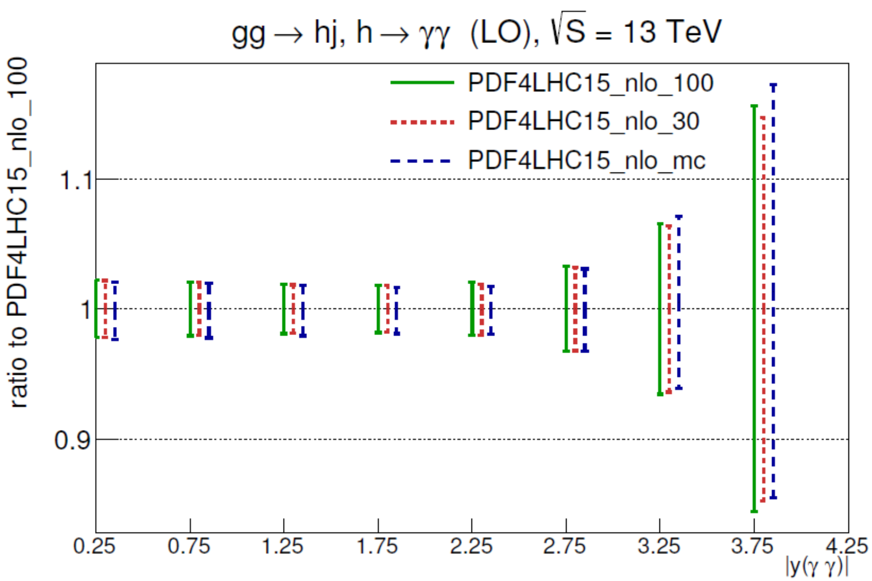

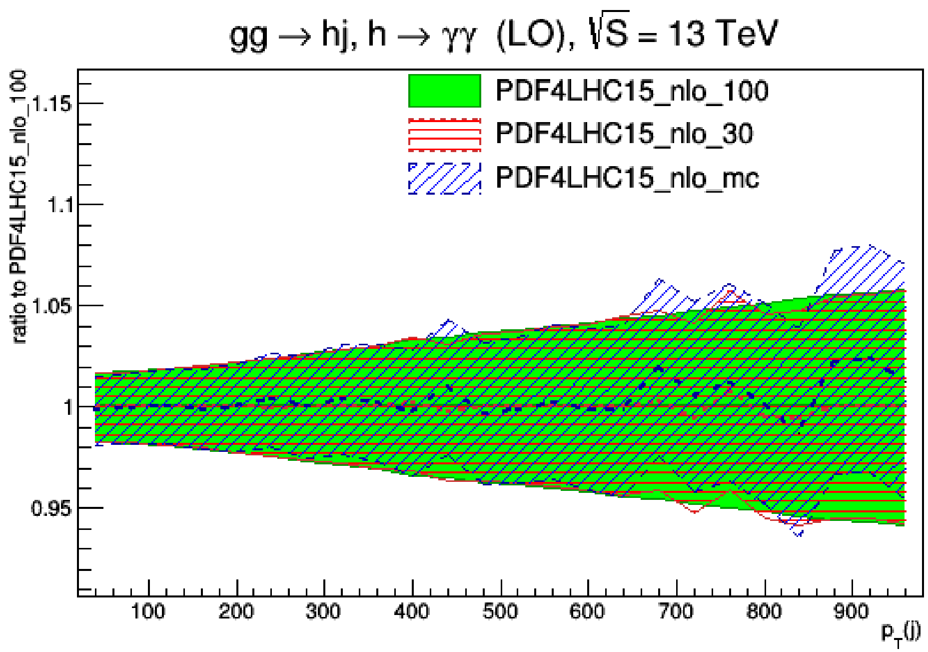

$gg \rightarrow H+j$ **at LO.**
10^6 events, ~1 hour per each PDF family

MC fluctuations in **central values** and PDF errors are often of the same order as the primordial differences

Higgs eigenvector set

- For a given class of observables, the _30 set can be **diagonalized** to reproduce the bulk of the uncertainties and correlations with ~6 eigenvector sets

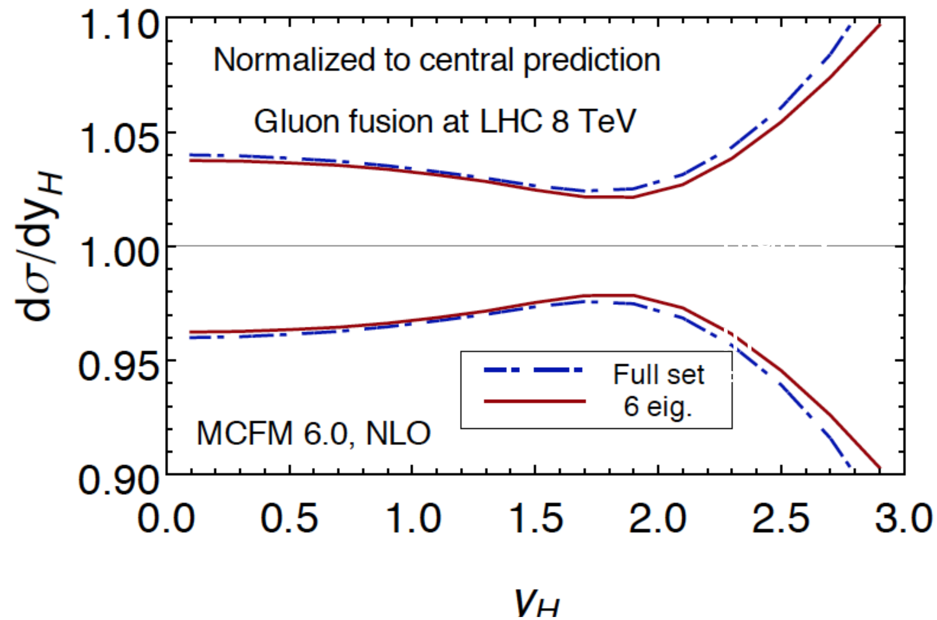

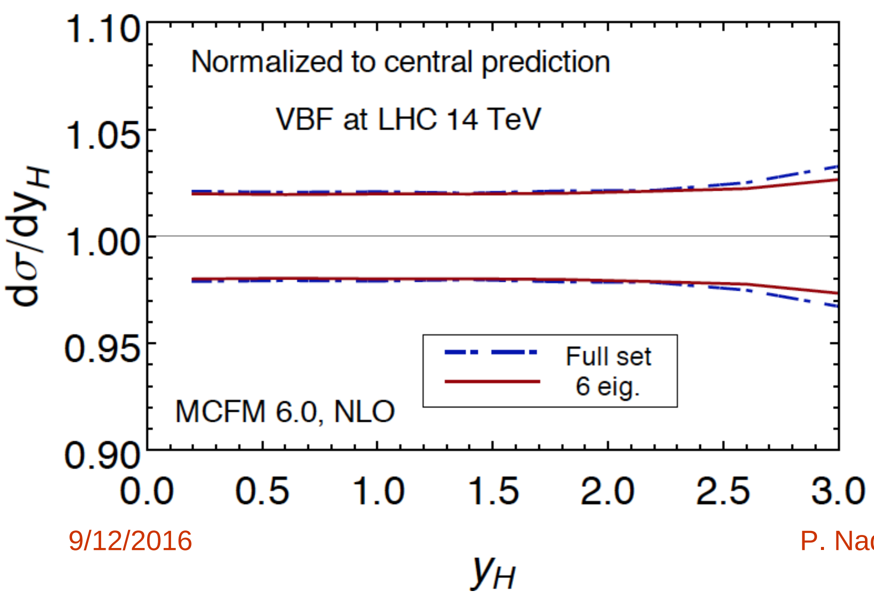

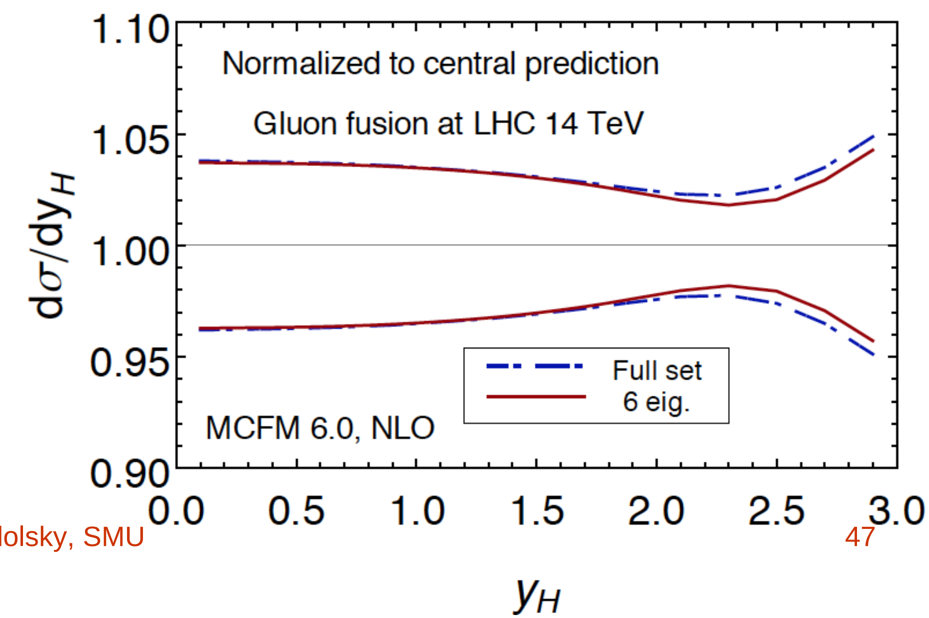

process	$\sigma_{cen.}$	δ_{Full}	$\delta_{Diag.}$	$\sigma^{\alpha_s}_{0.116}$	$\sigma^{\alpha_s}_{0.12}$
$gg \to H$ [pb]	18.77	$^{+0.48}_{-0.46}$	$^{+0.48}_{-0.44}$	18.11	19.4
	43.12	$^{+1.13}_{-1.07}$	$^{+1.13}_{-1.04}$	41.68	44.6
VBF [fb]	302.5	$^{+7.8}_{-6.7}$	$^{+7.6}_{-6.7}$	303.1	301.
	878.2	$^{+19.7}_{-17.9}$	$^{+19.2}_{-17.3}$	877.3	878.
HZ [fb]	396.3	$^{+8.4}_{-7.3}$	$^{+8.1}_{-7.4}$	393.0	399.
	814.3	$^{+14.8}_{-13.2}$	$^{+13.8}_{-13.0}$	806.5	823.
$HW^{\pm}$ [fb]	703.0	$^{+14.4}_{-14.4}$	$^{+14.3}_{-14.1}$	697.4	708.
	1381	$^{+28}_{-22}$	$^{+26}_{-22}$	1368	139
HH [fb]	7.81	$^{+0.33}_{-0.30}$	$^{+0.33}_{-0.30}$	7.50	8.1
	27.35	$^{+0.78}_{-0.72}$	$^{+0.78}_{-0.68}$	26.48	28.2
$t\bar{t}$ [pb]	248.4	$^{+9.1}_{-8.2}$	$^{+9.2}_{-8.1}$	237.1	259.
	816.9	$^{+21.4}_{-19.6}$	$^{+21.4}_{-18.4}$	785.5	848.
$Z/\gamma^*(l^+l^-)$ [nb]	1.129	$^{+0.025}_{-0.023}$	$^{+0.024}_{-0.023}$	1.113	1.14
	1.925	$^{+0.043}_{-0.041}$	$^{+0.040}_{-0.037}$	1.897	1.95
$W^+(l^+\nu)$ [nb]	7.13	$^{+0.14}_{-0.14}$	$^{+0.14}_{-0.13}$	7.03	7.2
	11.64	$^{+0.24}_{-0.23}$	$^{+0.22}_{-0.21}$	11.46	11.8
$W^-(l^-\bar{\nu})$ [nb]	4.99	$^{+0.12}_{-0.12}$	$^{+0.12}_{-0.11}$	4.92	5.0
	8.59	$^{+0.21}_{-0.20}$	$^{+0.19}_{-0.18}$	8.46	8.74
W^+W^- [pb]	4.14	$^{+0.08}_{-0.08}$	$^{+0.08}_{-0.07}$	4.04	4.2
	7.54	$^{+0.15}_{-0.14}$	$^{+0.14}_{-0.12}$	7.39	7.5
ZZ [pb]	0.703	$^{+0.016}_{-0.014}$	$^{+0.015}_{-0.014}$	0.695	0.71
	1.261	$^{+0.026}_{-0.024}$	$^{+0.024}_{-0.022}$	1.256	1.27
W^+Z [pb]	1.045	$^{+0.019}_{-0.018}$	$^{+0.019}_{-0.017}$	1.039	1.06
	1.871	$^{+0.033}_{-0.031}$	$^{+0.029}_{-0.027}$	1.850	1.89
W^-Z [pb]	0.788	$^{+0.020}_{-0.019}$	$^{+0.019}_{-0.018}$	0.780	0.79
	1.522	$^{+0.034}_{-0.032}$	$^{+0.033}_{-0.031}$	1.509	1.54

	GGH inc., 8 TeV, NNLO	GGH 0j exc., 8 TeV, NLO	GGH 1j exc., 8 TeV, NLO	GGH 2j inc., 8 TeV, LO	GGH 2j exc., 8 TeV, LO	GGH 2j full mass, 8 TeV, LO	VBF inc., 8 TeV, LO	VBF exc., 8 TeV, LO	GGH inc., 14 TeV, NNLO	GGH 0j exc., 14 TeV, NLO	GGH 1j exc., 14 TeV, NLO	GGH 2j inc., 14 TeV, LO	GGH 2j exc., 14 TeV, LO	GGH 2j full mass, 14 TeV, LO	VBF inc., 14 TeV, LO	VBF exc., 14 TeV, LO
VBF exc., 14 TeV, LO	−0.43 / ***−0.44***	−0.49 / ***−0.5***	−0.3 / ***−0.33***	0.09 / ***0.09***	0.09 / ***0.09***	0.06 / ***0.09***	0.92 / ***0.93***	0.92 / ***0.93***	−0.39 / ***−0.4***	−0.42 / ***−0.44***	−0.33 / ***−0.35***	0.02 / ***0.02***	0.02 / ***0.02***	0. / ***0.***	1. / ***1.***	
VBF inc., 14 TeV, LO	−0.43 / ***−0.44***	−0.49 / ***−0.5***	−0.3 / ***−0.33***	0.09 / ***0.09***	0.09 / ***0.09***	0.06 / ***0.09***	0.92 / ***0.93***	0.92 / ***0.93***	−0.39 / ***−0.4***	−0.42 / ***−0.44***	−0.33 / ***−0.35***	0.02 / ***0.02***	0.02 / ***0.02***	0. / ***0.***		
GGH 2j full mass, 14 TeV, LO	0.45 / ***0.42***	0.25 / ***0.22***	0.72 / ***0.71***	0.96 / ***0.98***	0.96 / ***0.98***	0.96 / ***0.98***	−0.04 / ***−0.05***	−0.04 / ***−0.05***	0.31 / ***0.28***	0.08 / ***0.05***	0.47 / ***0.46***	0.99 / ***0.99***	0.99 / ***0.99***			
GGH 2j exc., 14 TeV, LO	0.43 / ***0.44***	0.22 / ***0.23***	0.71 / ***0.72***	0.97 / ***0.98***	0.97 / ***0.98***	0.97 / ***0.98***	−0.01 / ***−0.02***	−0.01 / ***−0.02***	0.29 / ***0.29***	0.07 / ***0.07***	0.46 / ***0.48***	0.99 / ***0.99***				
GGH 2j inc., 14 TeV, LO	0.43 / ***0.44***	0.22 / ***0.23***	0.71 / ***0.72***	0.97 / ***0.98***	0.97 / ***0.98***	0.97 / ***0.98***	−0.01 / ***−0.02***	−0.01 / ***−0.02***	0.29 / ***0.29***	0.07 / ***0.07***	0.46 / ***0.48***					
GGH 1j exc., 14 TeV, NLO	0.98 / ***0.98***	0.94 / ***0.94***	0.93 / ***0.94***	0.3 / ***0.33***	0.3 / ***0.33***	0.3 / ***0.33***	−0.34 / ***−0.34***	−0.34 / ***−0.34***	0.97 / ***0.97***	0.89 / ***0.9***						
GGH 0j exc., 14 TeV, NLO	0.91 / ***0.92***	0.96 / ***0.97***	0.7 / ***0.73***	−0.07 / ***−0.08***	−0.07 / ***−0.08***	−0.07 / ***−0.08***	−0.4 / ***−0.4***	−0.4 / ***−0.4***	0.97 / ***0.97***							
GGH inc., 14 TeV, NNLO	0.97 / ***0.97***	0.97 / ***0.98***	0.84 / ***0.87***	0.14 / ***0.14***	0.14 / ***0.14***	0.14 / ***0.14***	−0.38 / ***−0.39***	−0.38 / ***−0.39***								
VBF exc., 8 TeV, LO	−0.41 / ***−0.41***	−0.44 / ***−0.45***	−0.31 / ***−0.33***	0.06 / ***0.05***	0.06 / ***0.05***	0.04 / ***0.05***	1. / ***0.99***									
VBF inc., 8 TeV, LO	−0.41 / ***−0.41***	−0.44 / ***−0.45***	−0.31 / ***−0.33***	0.06 / ***0.05***	0.06 / ***0.05***	0.04 / ***0.05***										
GGH 2j full mass, 8 TeV, LO	0.27 / ***0.29***	0.06 / ***0.08***	0.57 / ***0.6***	0.99 / ***0.99***	0.99 / ***0.99***											
GGH 2j exc., 8 TeV, LO	0.27 / ***0.29***	0.06 / ***0.08***	0.57 / ***0.6***	0.99 / ***0.99***												
GGH 2j inc., 8 TeV, LO	0.27 / ***0.29***	0.06 / ***0.08***	0.57 / ***0.6***													
GGH 1j exc., 8 TeV, NLO	0.93 / ***0.93***	0.83 / ***0.83***														
GGH 0j exc., 8 TeV, NLO	0.97 / ***0.97***															
GGH inc., 8 TeV, NNLO	3.3% / ***3.3%***	3.2% / ***3.2%***	3.6% / ***3.5%***	6.9% / ***6.8%***	6.9% / ***6.8%***	7.% / ***6.8%***	2.4% / ***2.4%***	2.4% / ***2.4%***	3.3% / ***3.3%***	3.2% / ***3.2%***	3.4% / ***3.4%***	5.7% / ***5.7%***	5.7% / ***5.7%***	5.8% / ***5.8%***	2.1% / ***2.%***	2.1% / ***2.%***

Correlation table for Higgs cross sections

Red indicates $|\cos(\phi)|>0.7$

Numbers in Italic–bold (plain) for 6 eigenvecotrs (full set 50 eig.)

META PDF 1.0 (LHCH)

VBF–like cut applied for 2 or more jets final states

jet (anti-k_T, 0.4) selection with $|y|<4.5$ and $p_T>30$ GeV

including α_s uncertainty

FIG. 7: Same as Fig. 5, with α_s uncertainties included by adding in quadrature.

Scouring the Horizon in 2016

High-luminosity LHC

- New (N)NNLO calculations likely to be completed
- Measurements of Higgs cross sections/couplings become limited by PDFs in the HL-LHC era
- Searches for non-resonant production in TeV mass range will demand accurate predictions for **sea** PDFs at $x > 0.1$
- The target is to obtain PDFs that "achieve 1% accuracy for LHC predictions" within about a decade

Projected Experimental Uncertainties

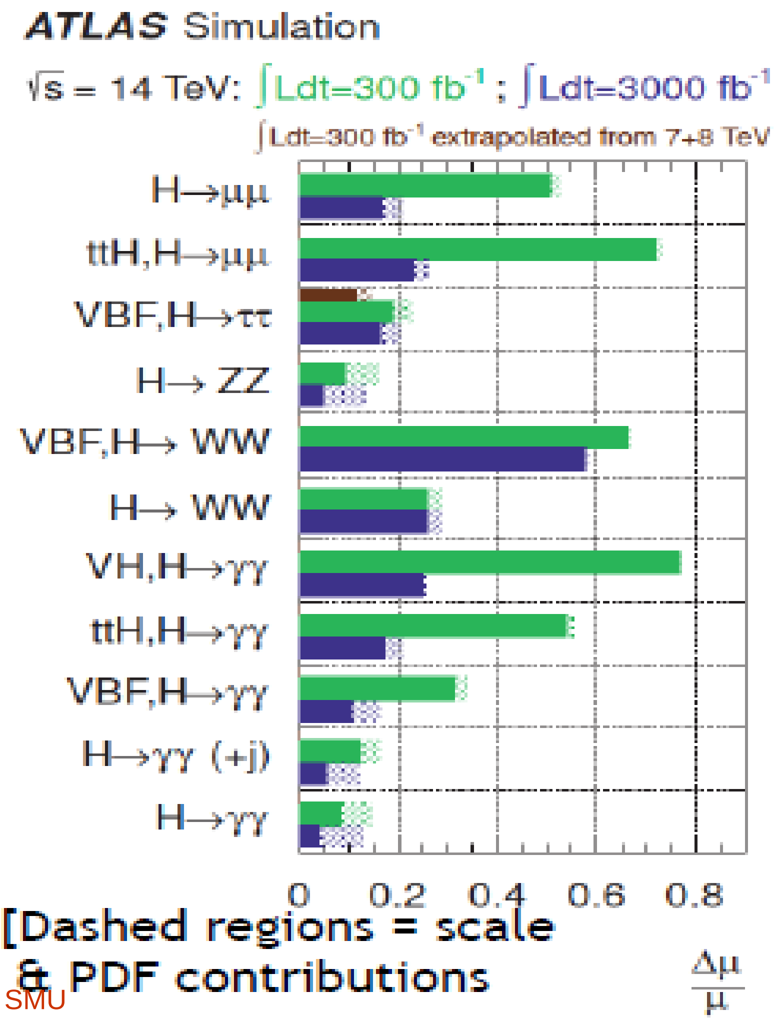

[Dashed regions = scale & PDF contributions

P. Newman, DIS'2016

Toward proton PDFs at 1% accuracy

Theory:

1. Development of efficient techniques to estimate PDF dependence at (N)NNLO
   a) Interfaces for fast (N)NLO computations *(Applgrid, FastNLO, aMCFast)*
   b) Combination at the PDF level *(META, CMC), reduced PDFs for classes of processes*
2. Inclusion of subleading effects (NLO EM corrections, photon PDFs, off-shell resonant production…) and theoretical uncertainties (scale dependence, heavy-quark schemes, …)
3. Special-purpose PDFs: for resummations, parton showering programs, with intrinsic charm,…
4. Advanced statistical methods (MC, reweighting…)

Toward proton PDFs at 1% accuracy

Experiment:

1. Finding new, highly sensitive measurements for constraining PDFs
   a) Less inclusive, yet clean, processes *(e.g.* $Z\ \ p_T$ *at NNLO…)*
   b) Better constraints at x>0.3
   c) Reliable flavor separation
2. Cross calibration of systematic uncertainties between the measurements
3. Smaller bin sizes, with some loss in statistics ⇒ better resolution on PDF x dependence

Usage

1. Recommendations for efficient use of PDFs in practical applications
2. Compression of relevant information available in multiple available PDF ensembles
3. Combination of PDFs at the level of parametrizations; PDF4LHC15 combined PDFs from global fits

NOW I AM READY FOR QUESTIONS

Backup slides

MMHT refit including combined HERA I+II data. Under refitting in global fit NLO – $\chi^2 = 1533/1185 = 1.29$ per point. NNLO – $\chi^2 = 1457/1185 = 1.23$ per point.

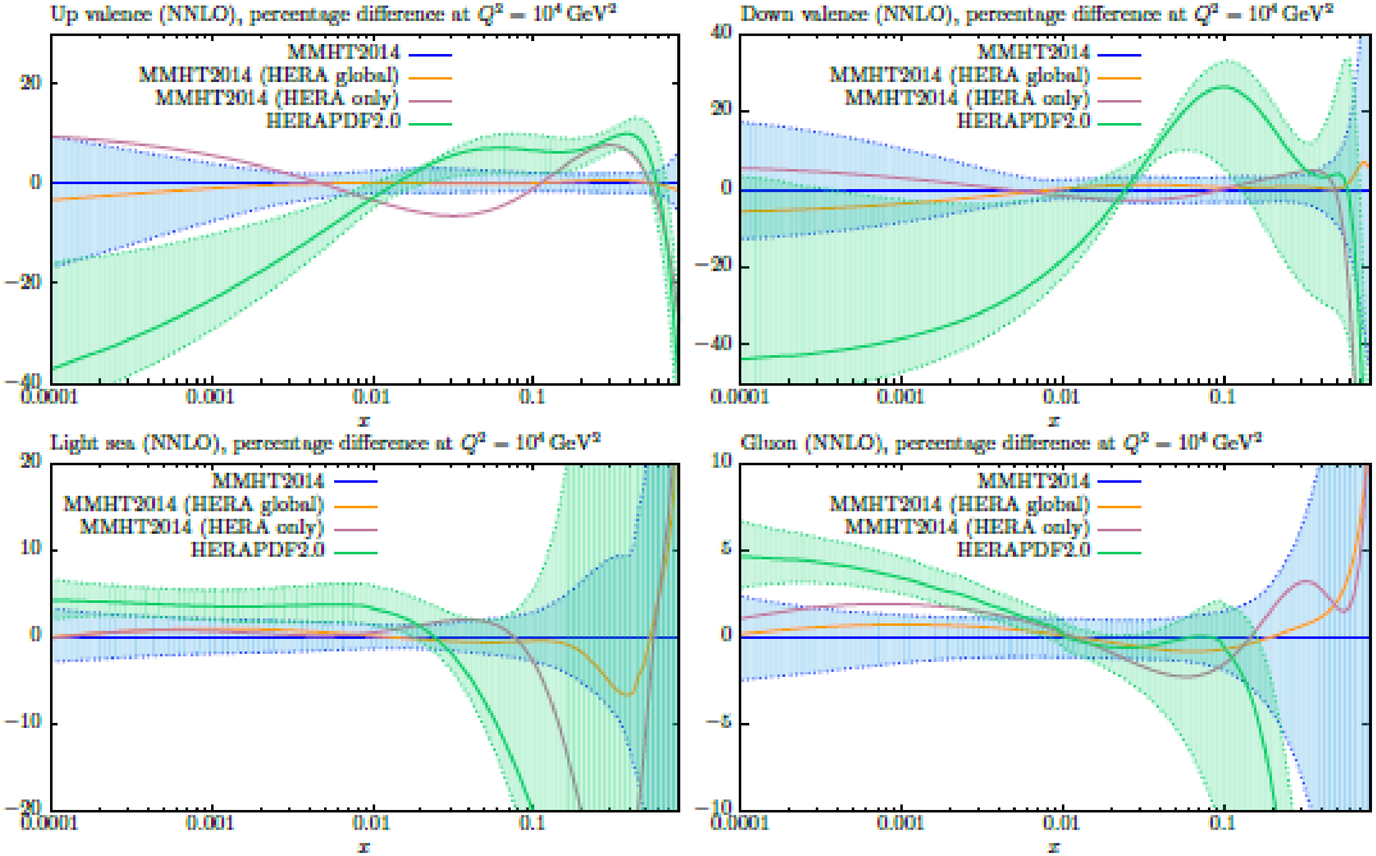

HERA II modified PDFs very well within MMHT2014 uncertainties. PDFs from HERA II data only fit in some ways similar to HERAPDF2.0.

R. Thorne

Modifications to the HERAPDF2.0 fit called HHT

By I.Abt, **A.M.Cooper-Sarkar**, B.Foster, V.Myronenko, K.Wichmann, M.Wing

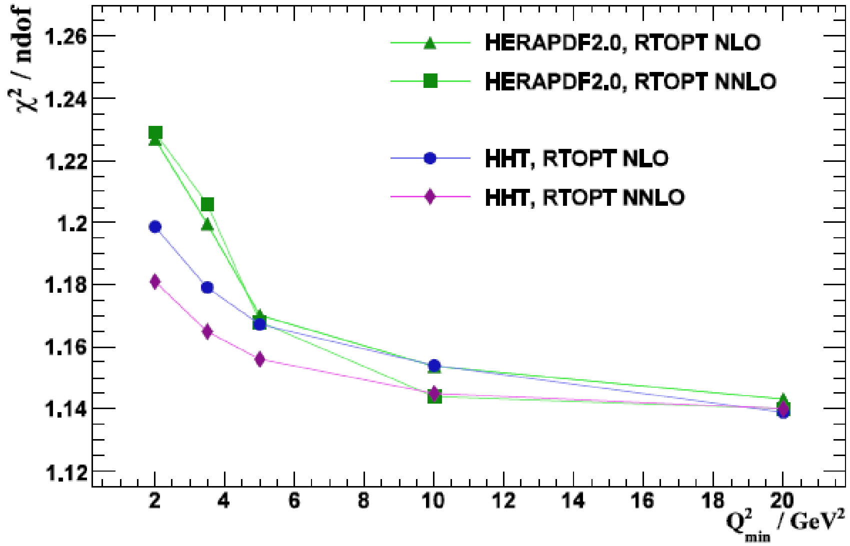

$$F_{2,L} = F_{2,L}\,(1 + A_{2,L}^{HT}/Q^2)$$

Addition of Higher Twist terms

- requires only modification of F_L
- and is only important for low-x

Greatly improves the description of low-Q^2, low-x and high-y data particularly at NNLO

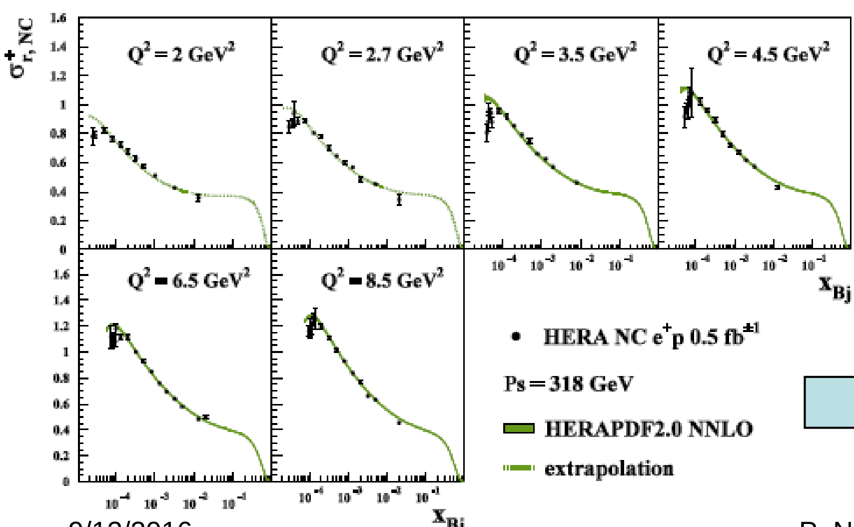

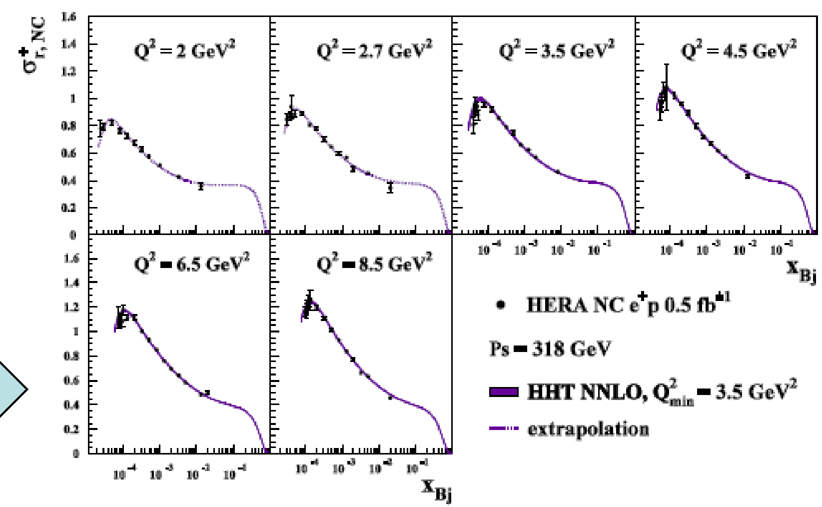

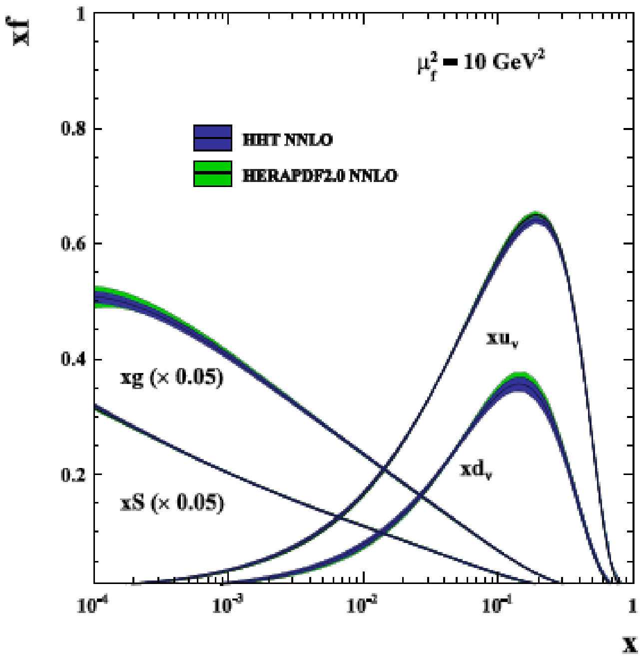

PDFs – and hence high Q^2 physics - not changed

Predicted FL - compared to the measured FL from H1 and ZEUS – is enhanced for $Q^2 < 50$ GeV^{2}.

However it is clear that this approach cannot be pushed to very low $Q^2 < \sim 2$ GeV^2

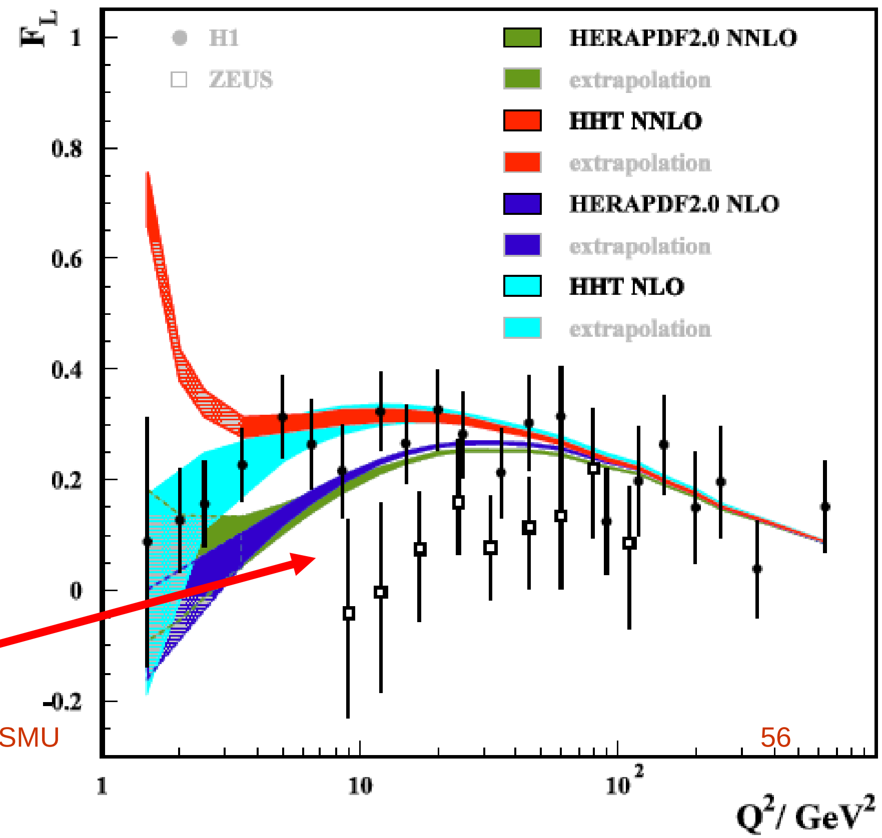

P.N.: Notice differences between H1 and ZEUS

Specialized PDF sets

CJ15: DIS data for $Q^2 > 1.3\ GeV^2$, $W^2 > 3\ GeV^2$

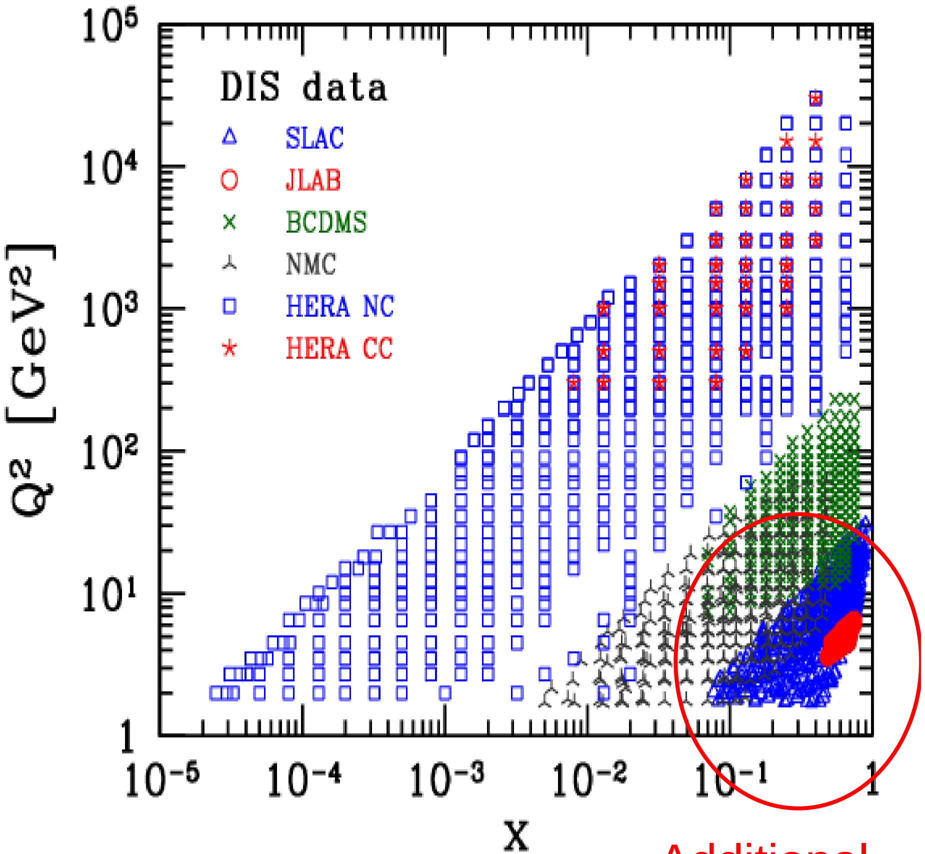

Additional constraints on d/u

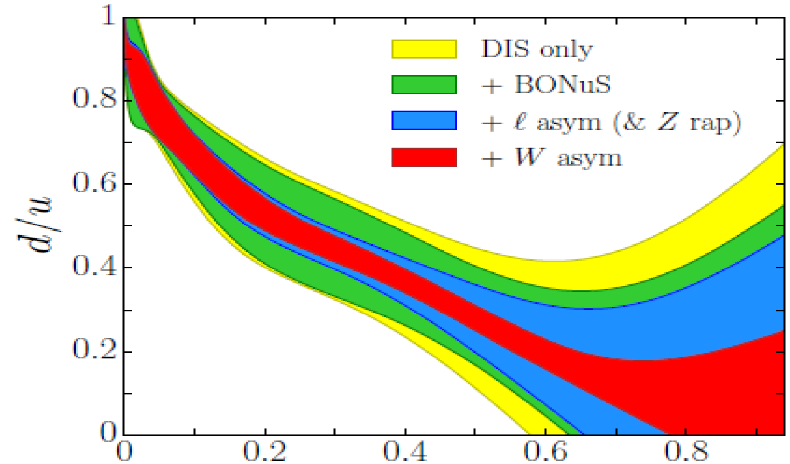

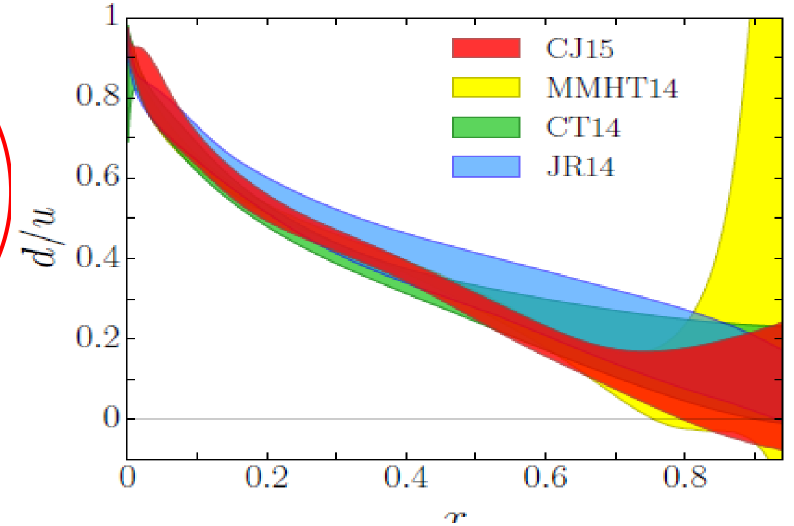

FIG. 16: Comparison of the d/u ratio at $Q^2 = 10\ \text{GeV}^2$ for different PDF parametrizations: CJ15 (red band), MMHT14 [6] (yellow band), CT14 [7] (green band), and JR14 [10] (blue band).

CJ15 vs. others

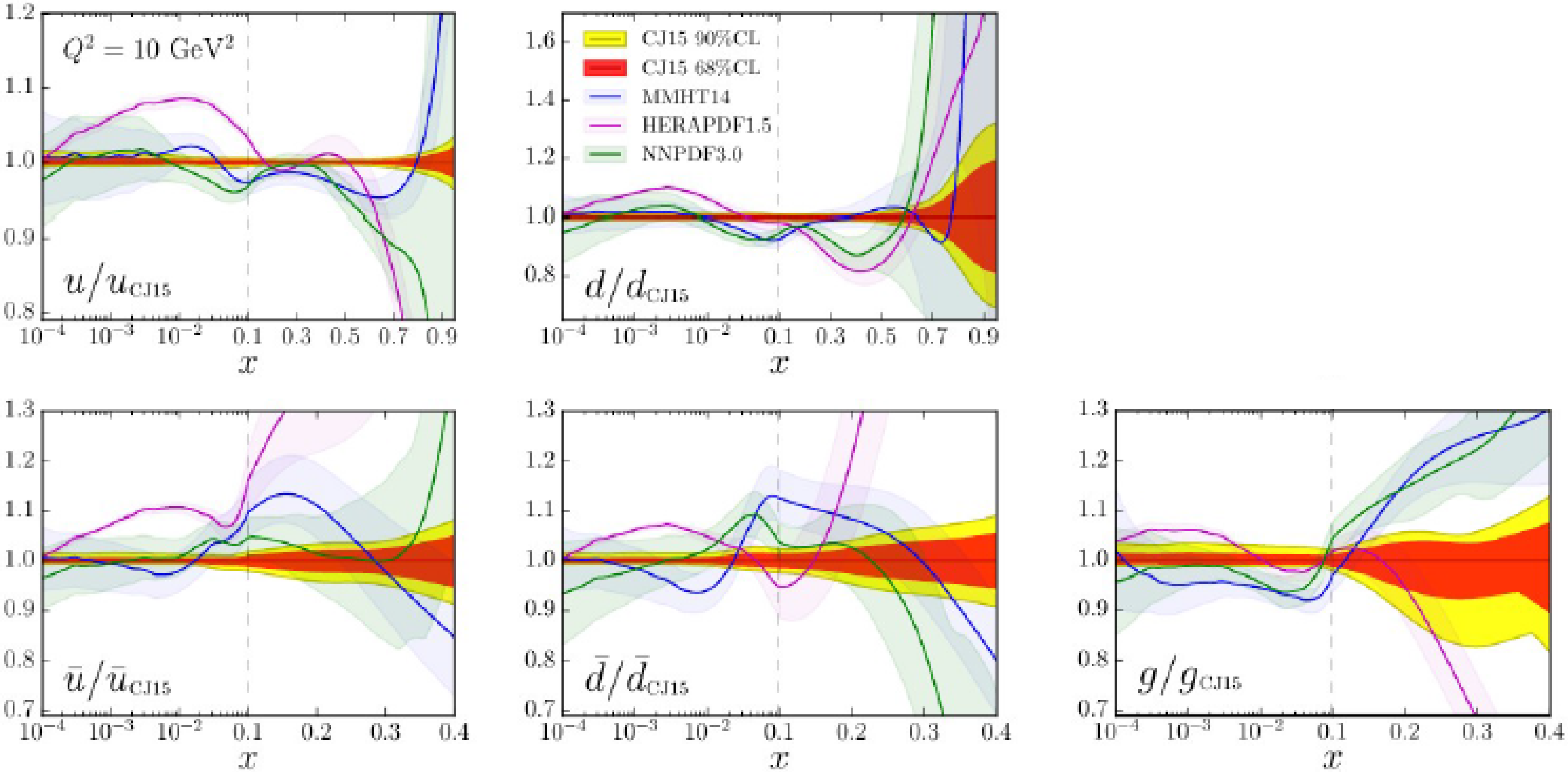

Intrinsic Charm PDFs from CTEQ-TEA Global Analysis

S. Dulat et al., 1309.0025; PoS DIS2015 (2015) 166

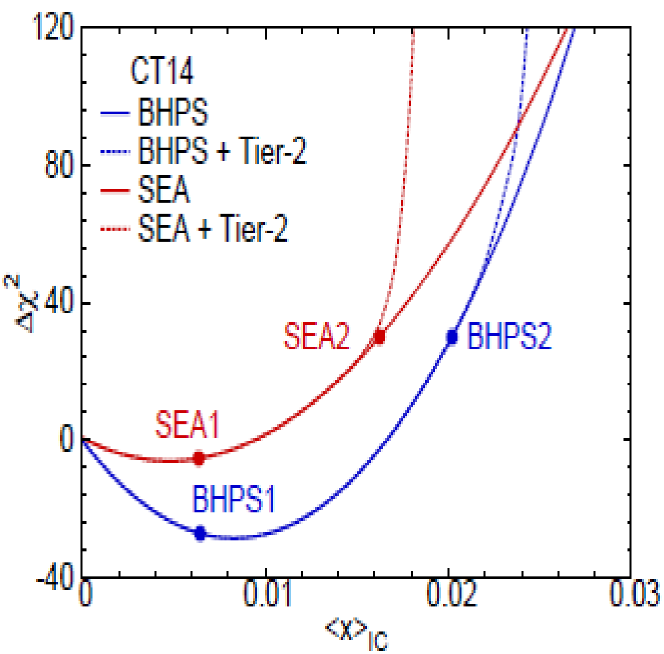

Figure 1: The $\Delta\chi^2$ versus the momentum fraction of charm $\langle x\rangle_{IC}$.

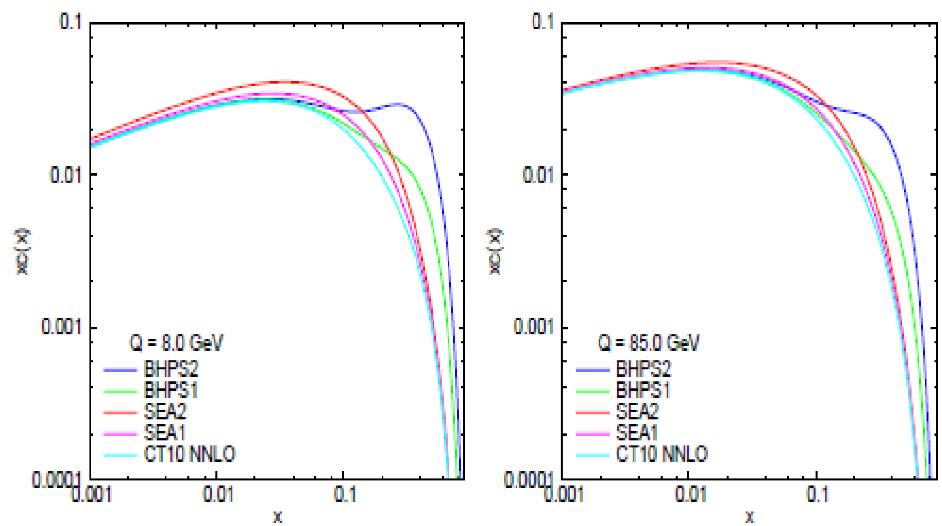

Ꞁ. 3: Charm quark distribution $x\,c(x,Q)$ from the BHPS1 and BHPS2 PDFs (which have 0.57% and 2% $\langle x\rangle_{\rm IC}$); from SEA1 and SEA2 PDFs (which have 0.57% and 1.5% $\langle x\rangle_{\rm IC}$); and from CT10.

News from NNPDF (II)

- First determination of the **fitted charm PDF** in the NNPDF framework
- **Non-perturbative charm** can account for **up to 0.8% of the proton momentum** (68% CL)
- The EMC **charm structure function data** can be satisfactorily described
- Fitting the charm PDF stabilises the **m_c dependence of high-scale cross-sections**

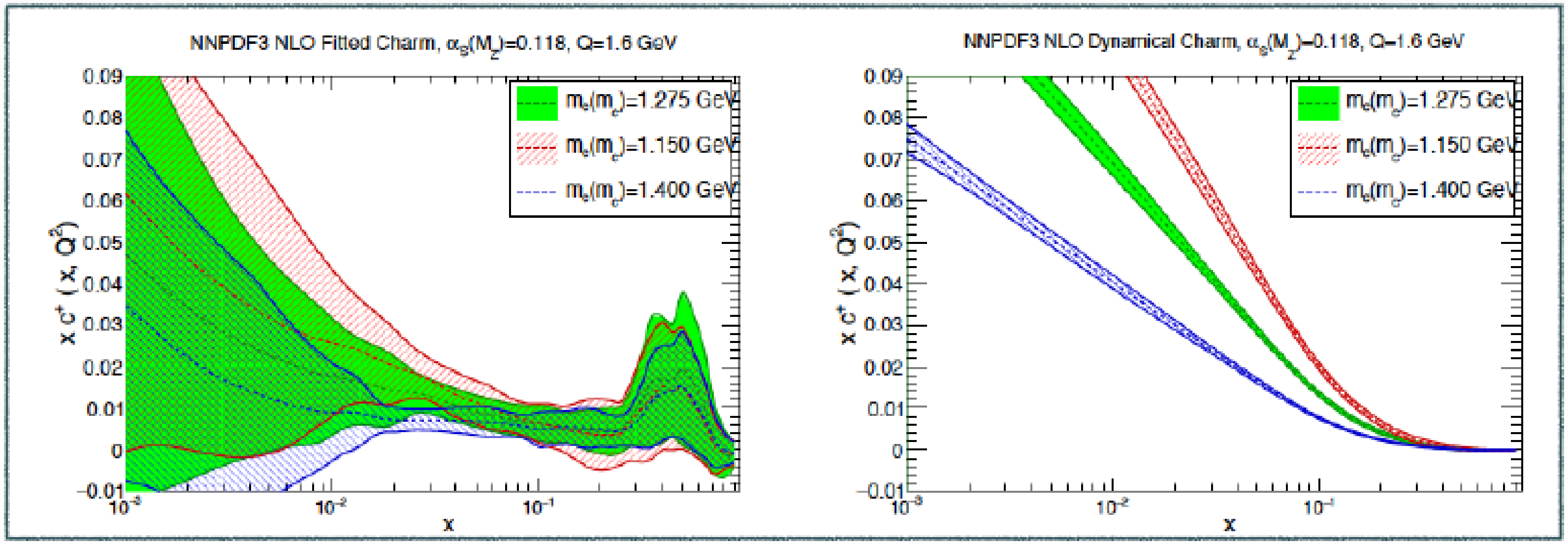

More in the talks from Juan Rojo (Tue) and Luca Rottoli (Wed)

Origin of increased tolerance

Error analysis: unique parametric model, compatible experiments

Treating each PDF value $f_a(x_b, Q_c)$ as a parameter a_i:

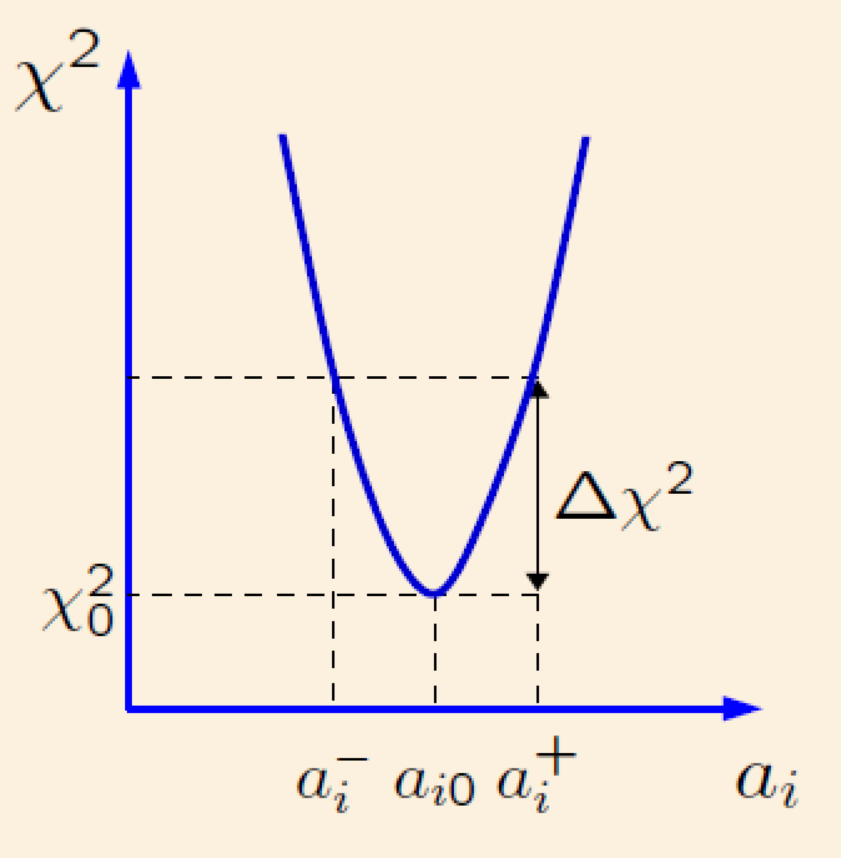

- Establish a confidence region for $\{a_i\}$ for a given tolerated increase in χ^2
- In the ideal case of perfectly compatible Gaussian errors, 68% c.l. on a physical observable X corresponds to $\Delta\chi^2 = 1$ independently of the number N of PDF parameters

See, e.g., P. Bevington, K. Robinson, Data analysis and error reduction for the physical sciences

Error analysis: multiple parametric models, somewhat incompatible experiments

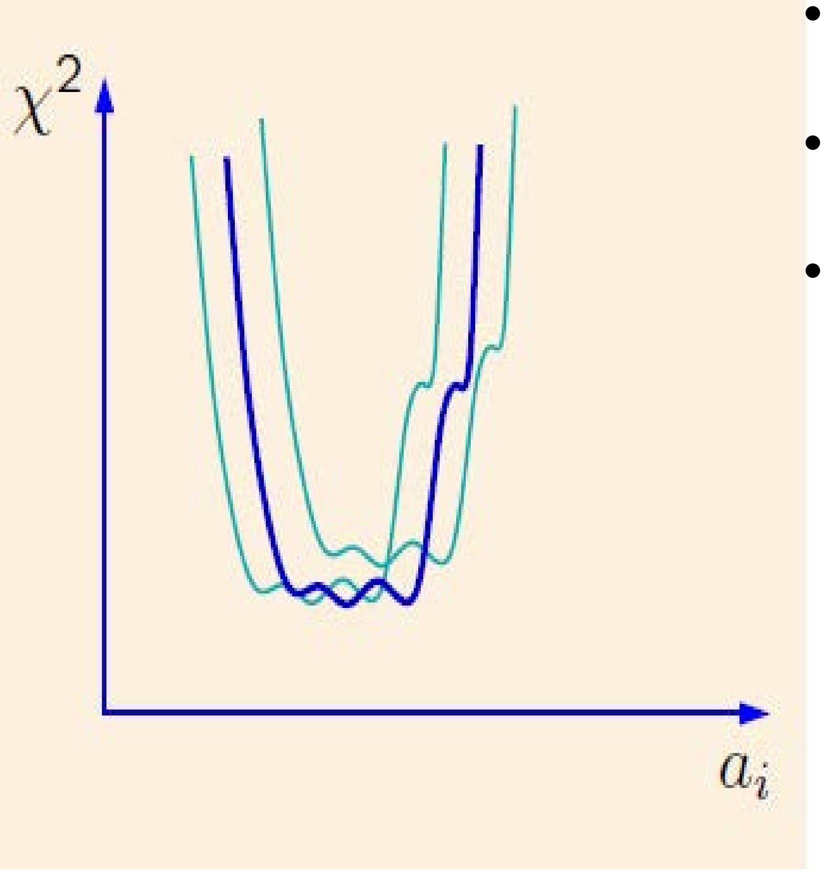

The actual χ^2 function shows

- a well-pronounced global minimum χ_0^2
- mild tensions between experiments (a mini-landscape)
- Dependence on the parametrization model and theoretical inputs (which ones?)

Error analysis: multiple parametric models, somewhat incompatible experiments

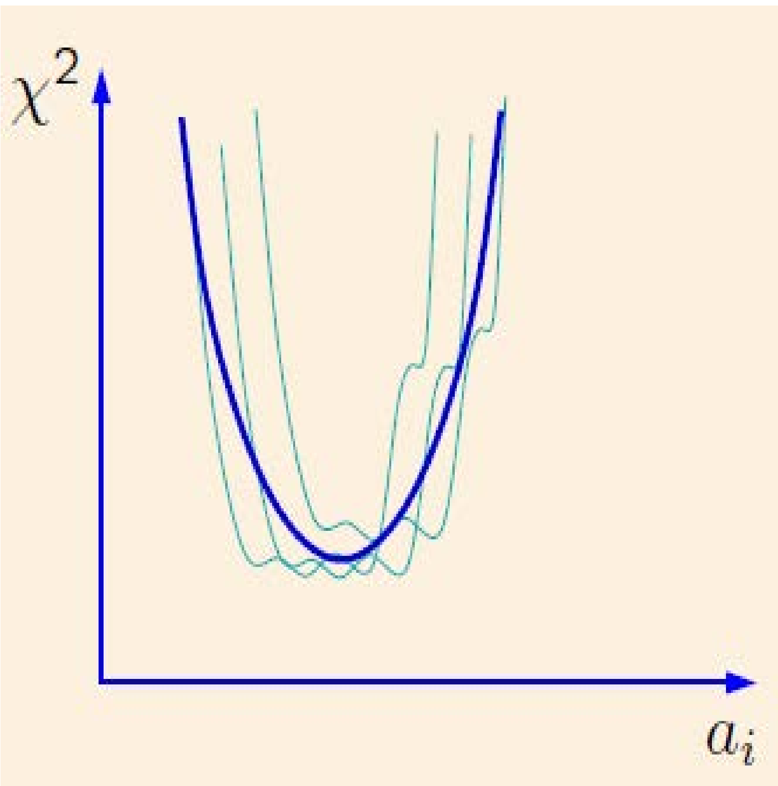

The actual χ^2 function shows

- a well-pronounced global minimum χ_0^2
- mild tensions between experiments (a mini-landscape)
- Dependence on the parametrization model and theoretical inputs (which ones?)

- The likelihood is approximately described by a quadratic χ^2 with a revised tolerance condition $\Delta\chi^2 \leq T^2$

Error analysis: multiple parametric models, somewhat incompatible experiments

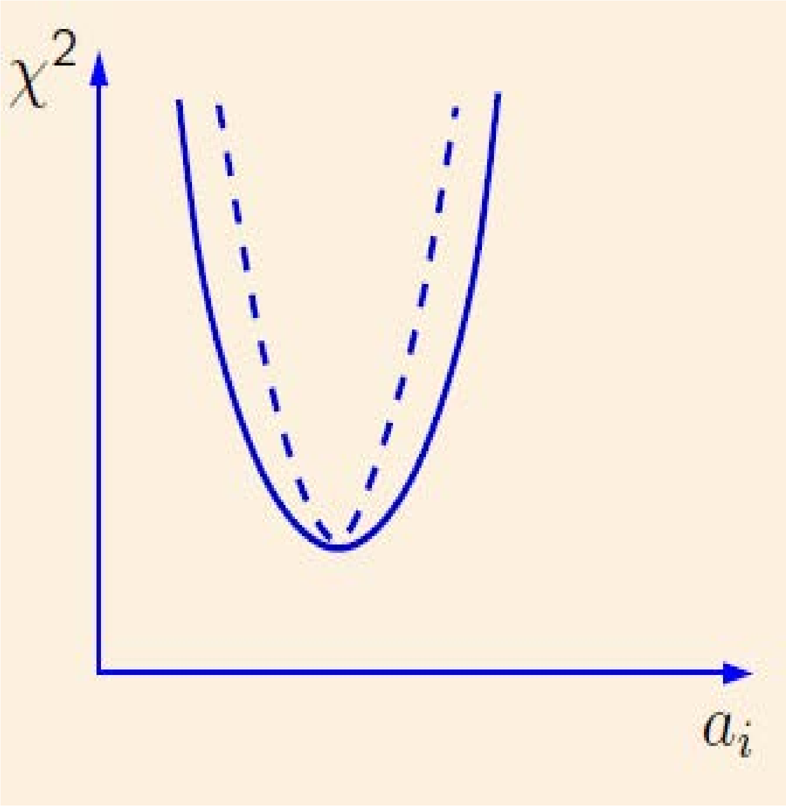

The actual χ^2 function shows

- a well-pronounced global minimum χ_0^2
- mild tensions between experiments (a mini-landscape)
- Dependence on the parametrization model and theoretical inputs (which ones?)

- The likelihood is approximately described by a quadratic χ^2 with a revised tolerance condition $\Delta\chi^2 \leq T^2$

Error analysis: multiple parametric models, somewhat incompatible experiments

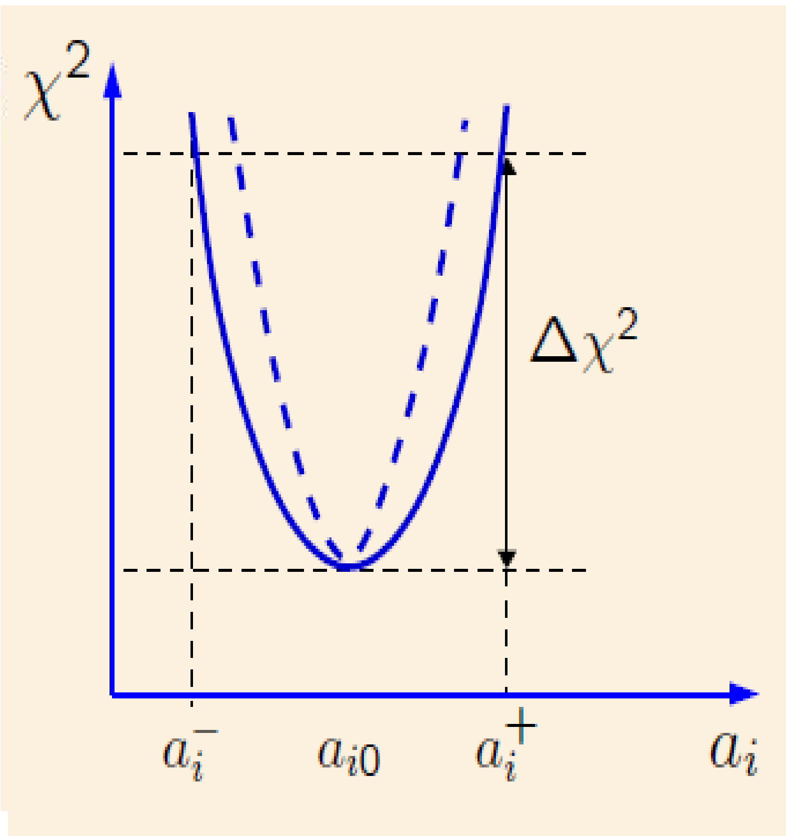

Tensions between experiments can be accommodated by choosing $T \sim 2-3$ (H. L. Lai et al., 1007.2241; Pumplin, 0909.0268)

Theory uncertainties reduce at NNLO; some residual theory errors can be accounted as systematic nuisance parameters

⇒ Progress depends on improved understanding of parametrization uncertainty

⇒ In the context of PDF reweighting, understanding of tolerance will lead to the proper construction of replica weights

Charm mass dependence of PDFs

Reduced META sets

2012→2015: Agreement between global NNLO PDFs greatly improved

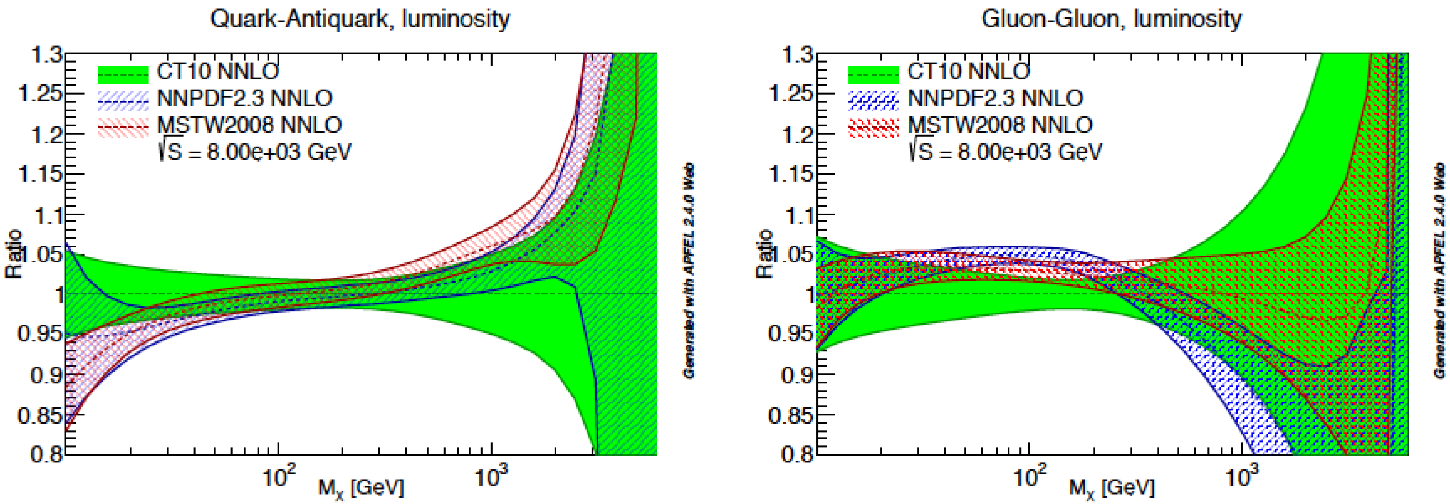

Figure 1: Comparison of the $q\bar{q}$ (left) and gg (right) PDF luminosities at the LHC 8 TeV for CT10, MSTW2008 and NNPDF2.3. Results are shown normalized to the central value of CT10

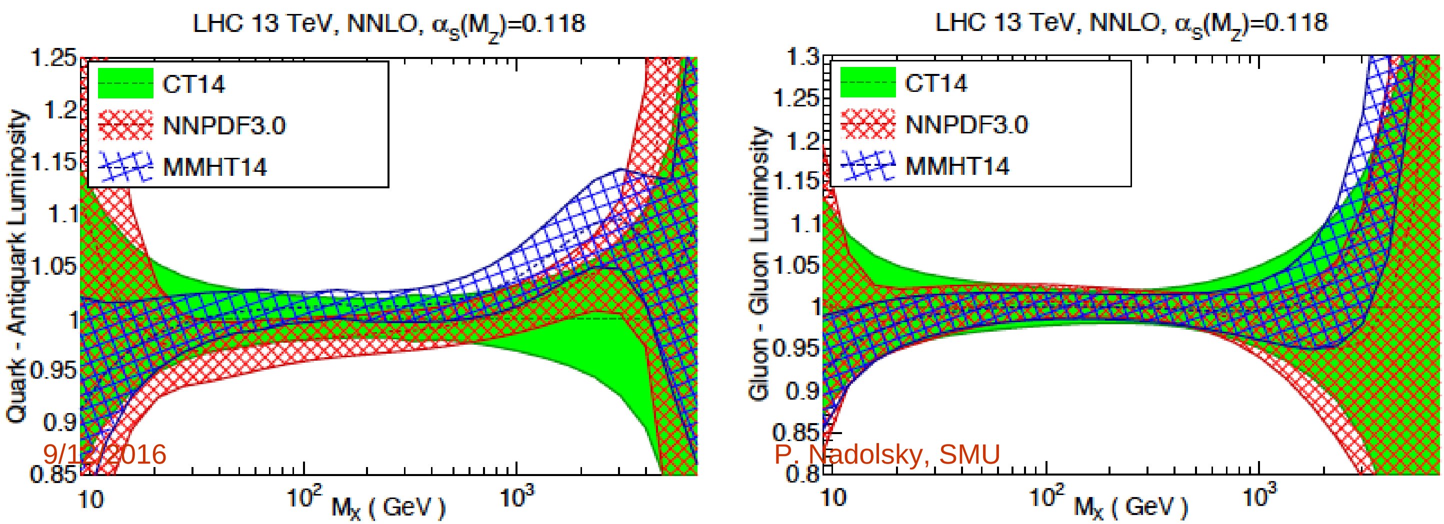

Note in particular the changes in the gg luminosity, especially important in the Higgs mass region

LHC data has been added for all 3 new PDFs, but most changes are due to benchmarking of formalisms

Why global NNLO PDFs are in better agreement now than ever

To start, various NNLO calculations have reduced dependence on renormalization, factorization, and auxiliary mass scales than at NLO

Since 2012, PDF analysis groups carried out a series of benchmarking exercises for key processes of DIS and jet production in PDF fits

Methodologies of all groups were cross-validated and improved.

Three main uses of PDFs at the LHC

1. Assessment of the *total uncertainty on a cross section* based on the available knowledge of PDFs, *e.g.*, when computing the cross section for a process that has not been measured yet (such as supersymmetric particle production cross-sections), or for estimating acceptance corrections on a given observable. This is also the case of the measurements that aim to verify overall, but not detailed, consistency with Standard Model expectations, such as when comparing theory with Higgs measurements.

2. Assessment of the accuracy of the *PDF sets themselves* or of related Standard Model parameters, typically done by comparing theoretical predictions using individual PDF sets to the most precise data available.

3. Input to the *Monte Carlo event generators* used to generate large MC samples for LHC data analysis.

For 2), compute cross sections with individual PDF sets.

For 1) or 3), the PDF uncertainty based on the totality of available PDF sets must be estimated. Estimate the combined PDF error using **an average of various PDF sets.**

Follow-up publications
In 2015 Les Houches proceedings

Address questions not covered in the main document of 2015 PDF4LHC recommendation (**arXiv:1510.03865**), and provide illustrations

***1*. Phenomenological applications of PDF4LHC distributions**

J. Gao, T.-J. Hou, J. Huston, P. N., B. Wang, K. Xie, …

Physics issues, predictions for typical QCD cross sections

2. On the accuracy and Gaussianity of the PDF4LHC15 combined sets of parton distributions

S.Carrazza, S. Forte, Z. Kassabov, J. Rojo

Comparisons of PDF4LHC ensembles, non-Gaussian effects

Choosing the right PDF set for an LHC application

6.1 Delivery and guidelines

The PDF4LHC15 combined PDFs are based on an underlying Monte Carlo combination of CT14, MMHT14 and NNPDF3.0, denoted by MC900, which is made publicly available in three different reduced delivery forms:

- **PDF4LHC15_mc**: a *Monte Carlo PDF set* with $N_{rep} = 100$ replicas.
- **PDF4LHC15_30**: a *symmetric Hessian PDF set* with $N_{eig} = 30$ eigenvectors.
- **PDF4LHC15_100**: a *symmetric Hessian PDF set* with $N_{eig} = 100$ eigenvectors.

In the three cases, combined sets are available at NLO and at NNLO, for the central value of $\alpha_s(m_Z^2) = 0.118$. In addition, we provide additional sets which contain the central values for $\alpha_s(m_Z^2) = 0.1165$ and $\alpha_s(m_Z^2) = 0.1195$, and that can be used for the computation of the combined PDF+α_s uncertainties, as explained in Sect. 6.2. Finally, for ease of usage, the combined sets for $\alpha_s(m_Z^2) = 0.118$ are also presented bundled with the α_s-varying sets in dedicated grid files. The specifications of each of the combined NNLO PDF4LHC15 sets that are available from LHAPDF6 are summarized in Table 5; note that the corresponding NLO sets are also available.

Usage of the PDF4LHC15 sets. As illustrated in Sect. 5, the three delivery options provide a reasonably accurate representation of the original prior combination. However, each of these methods has its own advantages and disadvantages, which make them more suited in different specific contexts. We now attempt to provide some general guidance about which of the three PDF4LHC15 combined sets should be used in specific phenomenological applications.

1. **Comparisons between data and theory for Standard Model measurements**

   Recommendations: Use *individual PDF sets*, and, in particular, as many of the modern PDF sets [5–11] as possible.

   Rationale: Measurements such as jet production, vector-boson single and pair production, or top-quark pair production, have the power to constrain PDFs, and this is best utilized and illustrated by comparing with many individual sets.

   As a rule of thumb, *any measurement that potentially can be included in PDF fits* falls in this category.

   The same recommendation applies to the *extraction of precision SM parameters*, such as the strong coupling $\alpha_s(m_Z^2)$ [75, 124], the W mass M_W [125], and the top quark mass m_t [126] which are directly correlated to the PDFs used in the extraction.

2. **Searches for Beyond the Standard Model phenomena**

   Recommendations: Use the PDF4LHC15_mc sets.

   Rationale: BSM searches, in particular for *new massive particles in the TeV scale*, often require the knowledge of PDFs in regions where available experimental constraints are limited, notably close to the hadronic threshold where $x \to 1$ [127]. In these extreme kinematical regions the PDF uncertainties are large, the *Monte Carlo combination of PDF sets is likely to be non-Gaussian*. *c.f.* Figs. 10 and 11.

47

The PDF4LHC document contains detailed guidelines to help decide which individual or combined PDFs to use depending on the circumstances

To assist in choosing the best PDF(s), demonstrative comparisons were generated of typical LHC cross sections for recent PDFs

1. **MC2H gallery of LHC cross sections:** ApplGrid, typical experimental cuts

www.hep.ucl.ac.uk/pdf4lhc/mc2h-gallery/

2. META gallery of LHC cross sections: ApplGrid or full calculations, minimal cuts

Metapdf.hepforge.org/2016_pdf4lhc/

NLO=$O(\alpha_s)$: GM-VFN predictions **for DIS** have large dependence on matching scales

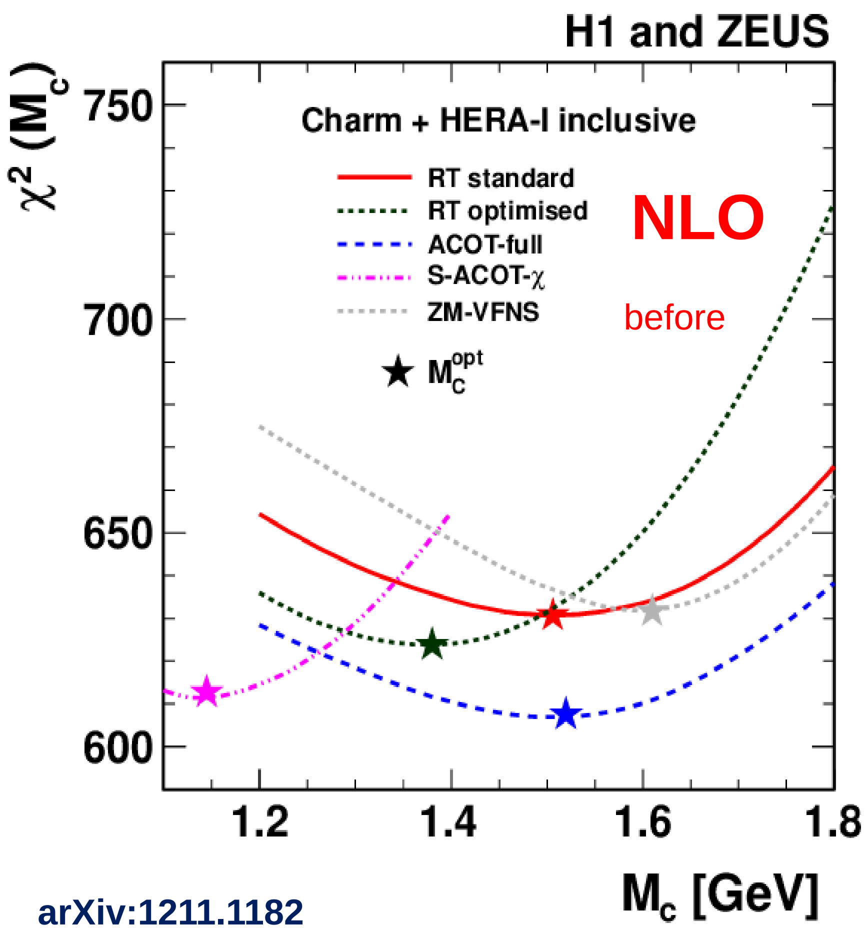

arXiv:1211.1182

The gluon PDF depends on the factorization scheme used to fit HERA DIS data

Besides the physical mass m_c, general-mass (GM-VFN) schemes used by global fits introduce matching energy scales of order m_c

At NLO, uncertainty due to matching parameters is large; each scheme prefers an "optimal" m_c that brings χ^2 to comparable levels (cf. the figure)

NNLO=$O(\alpha_s^2)$: dependence on matching parameters is suppressed, GM-VFN schemes are more similar

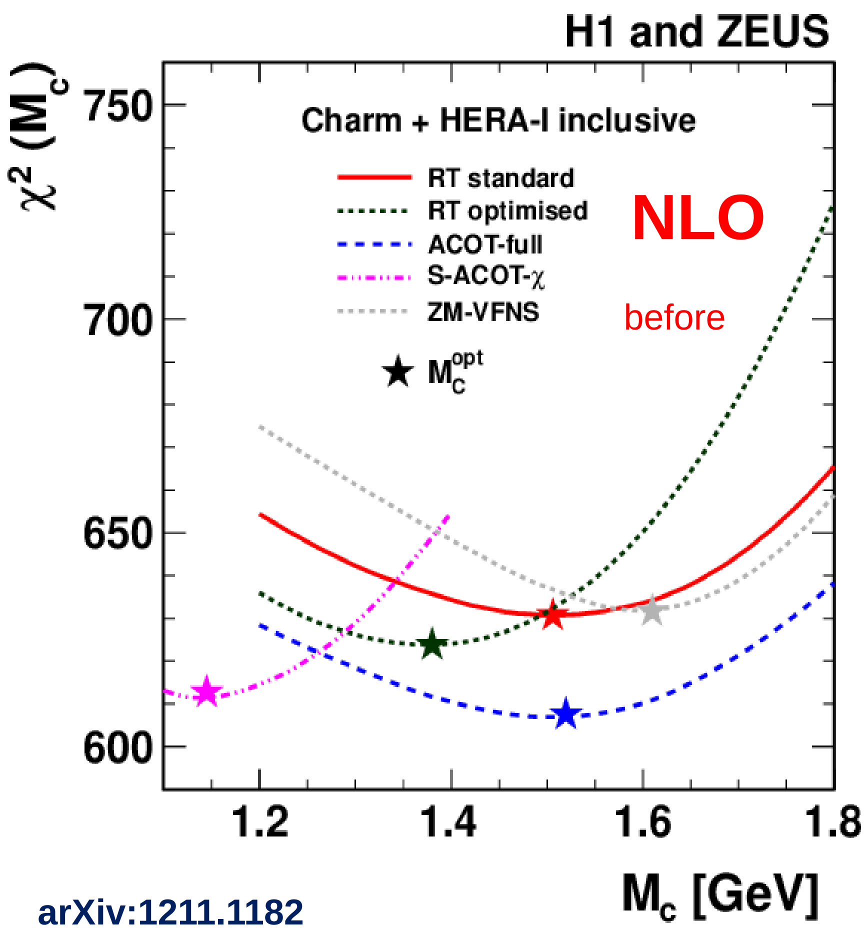

arXiv:1211.1182

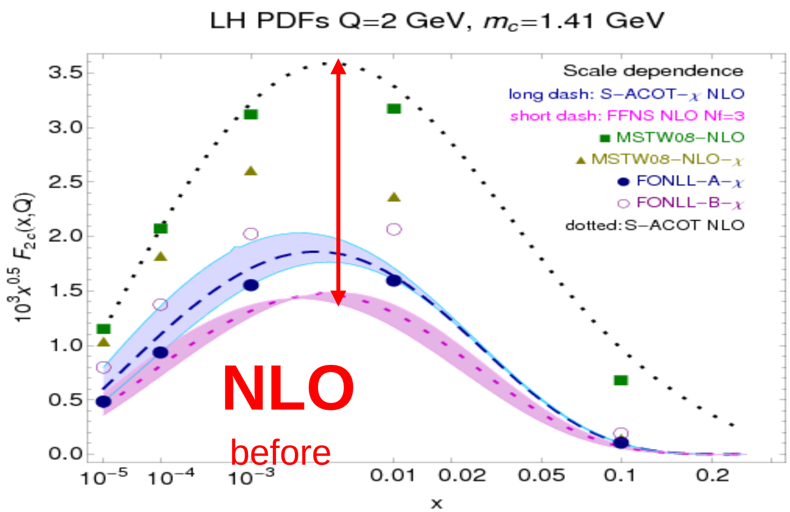

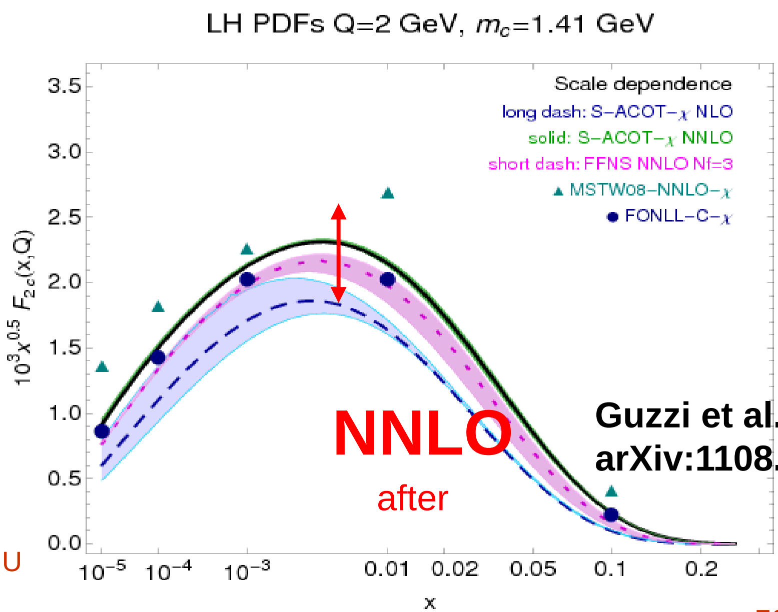

Guzzi et al.; arXiv:1108.5112

GM-VFN schemes are more predictive at NNLO

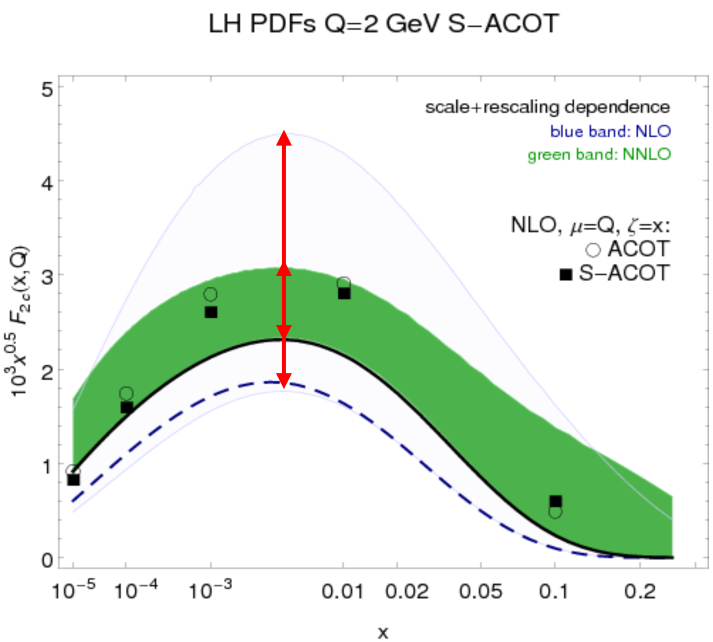

From Guzzi et al.; arXiv:1108.5112;
see also J. Rojo et al., 1003.1241, p. 110

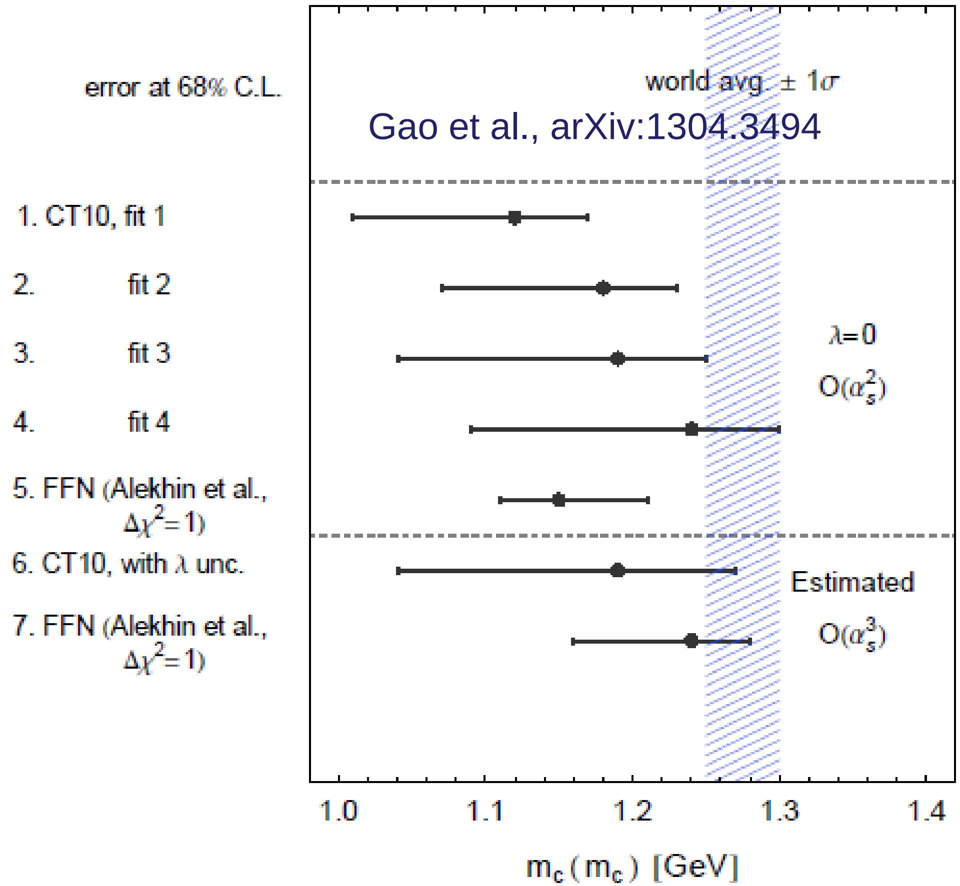

At $O(\alpha_s^2)$ and approximate $O(\alpha_s^3)$, constraints on $m_c(m_c)$ have been first obtained from combined HERA-I data in the FFN scheme (1212.2355) . Constraints on both m_c^{pole} or $m_c(m_c)$ in GM-VFNS have been also obtained by CT, MMHT, and NNPDF under varied assumptions. They are comparable with FFNS and the PDG value for $m_c(m_c)$.